2014

Quantification of Molecular Changes in the Brown bullhead (Ameiurus nebulosus) Exposed to Environmental Toxins

Rebecca A. Williams
University of Windsor

SCALE EFFECTS ON DESIGN ESTIMATION OF SCOUR DEPTHS AT PIERS

By

Priscilla D. Williams

A Thesis
Submitted to the Faculty of Graduate Studies
through the Department of Civil and Environmental Engineering
in Partial Fulfillment of the Requirements for
the Degree of Master of Applied Science
at the University of Windsor

Windsor, Ontario, Canada

2014

SCALE EFFECTS ON DESIGN ESTIMATION OF SCOUR DEPTHS AT PIERS

by

Priscilla D. Williams

APPROVED BY:

_____

D. Ting
Department of Mechanical, Automotive and Materials Engineering

_____

R. Carriveau
Department of Civil and Environmental Engineering

_____

T. Bolisetti, Advisor
Department of Civil and Environmental Engineering

_____

R. Balachandar, Advisor
Department of Civil and Environmental Engineering

April 15, 2014

DECLARATION OF PREVIOUS PUBLICATION

This thesis includes one (1) original paper that will be published/submitted for publication in peer reviewed journals, as follows:

Thesis Chapter	Publication title/full citation	Publication status*
Chapters 1-5	*P. Williams, R. Balachandar, and T. Bolisetti. (2014). "Scale Effects on Design Estimation of Scour Depths at Piers."*	*Not yet submitted*

I certify that the above material describes work completed during my registration as graduate student at the University of Windsor.

I certify that, to the best of my knowledge, my thesis does not infringe upon anyone's copyright nor violate any proprietary rights and that any ideas, techniques, quotations, or any other material from the work of other people included in my thesis, published or otherwise, are fully acknowledged in accordance with the standard referencing practices. Furthermore, to the extent that I have included copyrighted material that surpasses the bounds of fair dealing within the meaning of the Canada Copyright Act, I certify that I have obtained a written permission from the copyright owner(s) to include such material(s) in my thesis.

I declare that this is a true copy of my thesis, including any final revisions, as approved by my thesis committee and the Graduate Studies office, and that this thesis has not been submitted for a higher degree to any other University or Institution.

ABSTRACT

Due to the prevalence of bridge failures resulting from scour or scour-related complications, design of piers with respect to scour is prioritized by engineers. Current scour estimation methods typically over-predict scour depth, which results in uneconomical design. This tendency is partly due to the complexity of the scouring process, indicating that there are many aspects of scour which are still not well understood, and can also be attributed to scale effects in scour modelling. In this investigation, experimentation was completed in order to isolate the influences of governing non-dimensional parameters (relative coarseness and flow shallowness) on scour. Results from testing were then compared with results from previous investigations at the University of Windsor, and the influences of densimetric Froude number and separation velocity (representative of channel blockage) on scour were determined. A new scour estimation method based on these influences is presented and compared with methods used in current practice.

DEDICATION

To Dad, Mom, and Rebecca

ACKNOWLEDGEMENTS

I would like to express my deepest thanks to my supervisors, Dr. Ram Balachandar and Dr. Tirupati Bolisetti, for their continuous guidance, support, and patience over the past two years. I would also like to thank the members of my committee, Dr. Rupp Carriveau and Dr. David Ting, for their comments and suggestions.

I would also like to thank the members of the CFD discussion group, including Dr. Ronald Barron and Dr. Vesselina Roussinova, for their weekly insight and support.

I would like to extend my appreciation and gratitude to Mr. Matt St. Louis and Mr. Lucian Pop for their expertise and assistance in the Sedimentation and Scour Study lab.

My sincere thanks to my labmates, colleagues and friends: Carlo D'Alessandro, Sebastian Tejada, Dr. Peng Wu, Mehdi Heidari, and Vimaldoss Jesudhas, for their perspective, instruction, and help in the lab; Ahmad Al-Hayale, Ramit Saraswat, and Spencer Hsu, for helping with the heavy lifting; Craig Taylor and Jamie Smith, for their assistance in the lab; and Kiri McDermott-Berryman, Amy Hucal, and Emily Southcott for their friendship, encouragement and belief.

Finally, I would like to thank my parents, Lawrence and Josephine Williams, and my sister, Rebecca Williams, for their constant love, patience, and support.

TABLE OF CONTENTS

LIST OF TABLES

LIST OF FIGURES

LIST OF APPENDICES

LIST OF ABBREVIATIONS/SYMBOLS

a*	effective pier diameter (Froehlich equation, Sheppard-Melville equation)
Al	pier alignment factor
ASTM	American Society for Testing and Materials
b	flume or channel width
D	pier width
D/b	blockage ratio
D/d_{50}	relative coarseness
d_{50}	median sediment diameter
d_{se}	equilibrium scour depth
d_{se}/D	relative scour depth
d_x	sediment size of which subscript "x" percent is finer by weight
Eu	Euler number
Eu_d	Pier Euler number
F_d	densimetric Froude number
F_{ds}	densimetric Froude number based on separation velocity
Fr	Froude number
Fr_c	critical Froude number
Fr_s	Froude number based on separation velocity
g	gravitational acceleration
h	approach flow depth
h/D	flow shallowness
K_1	flow intensity parameter (Melville and Sutherland equation)

K_1	pier nose shape factor (HEC-18 equation)
K_2	angle of attack factor (HEC-18 equation)
K_3	bed condition factor (HEC-18 equation)
K_4	armoring condition factor (HEC-18 equation)
K_d	sediment size parameter (Melville and Sutherland equation)
K_s	pier shape parameter (Melville and Sutherland equation)
K_y	flow depth parameter (Melville and Sutherland equation)
K_α	pier alignment parameter (Melville and Sutherland equation)
K_σ	sediment gradation parameter (Melville and Sutherland equation)
Q	flow rate
Re	Reynolds number
SG	specific gravity
Sh	pier shape factor
SS	sum of least squares
St	Strouhal number
t_s	time to scour
t_{se}	time to equilibrium scour
U	mean approach flow velocity
U/U_c	flow intensity
U_c	critical velocity of bed material
U_s	velocity along streamline at point of separation on pier
w_s	width of scour hole
w_s/D	relative scour width

Θ	angle of attack of approach flow
λ	scale factor
μ	fluid dynamic viscosity
ν	fluid kinematic viscosity
ρ	fluid density
ρ_s	sediment density
σ_g	uniformity of particle size distribution
φ	pier nose shape factor (Froehlich equation)

CHAPTER 1

INTRODUCTION

1.1. Introduction

As a majority of engineering infrastructure in North America continues to near its service life, modern engineers are often faced with the necessity of monitoring and rehabilitating aging structures. Bridges are not an exception to this phenomenon; these structures are, indeed, highly susceptible to distress or collapse due to design flaws and external events (Wardhana and Hadipriono, 2003). **Table 1.1** demonstrates that several investigators have determined that scour or scour-related complications yield half (or in some cases, as high as 60 percent) of all bridge collapses in the United States (Melville and Coleman, 2000; Wardhana and Hadipriono, 2003; Foti and Sabia, 2011).

Table 1.1: Frequency of scour-related bridge failures in North America

Investigator(s)	Year	Number of failed bridges surveyed	Failures caused by scour
Shirhole and Holt	1991	823	**60%** (scour and scour-related complications)
Wardhana and Hadipriono	2003	500+	**53%** (flood and scour)
Briaud (as quoted by Miroff)	2007	1502	**60%** (scour around foundation)

There have been several high-profile bridge failures due to scour which have occurred over the past half-century. The most infamous of these is perhaps the Schoharie Creek bridge collapse, which took place in upstate New York in 1987. As a result of unanticipated spring flooding, rip-rap protection around the base of one of the bridge's

piers experienced failure, eventually causing collapse of three of the bridge's five spans (**Figure 1.1**). This incident resulted in ten deaths (LeBeau and Wadia-Fascetti, 2007).

Figure 1.1. Aftermath of Schoharie Creek bridge collapse (Chen, 2011: accessed from http://laser.umkc.edu/~chen/research%20projects.html)

A recent case of bridge failure due to scour took place in Alberta, Canada during spring flooding in June of 2013. A Canadian Pacific railroad bridge collapsed over the Bow River in Calgary, resulting in derailment of six train cars (**Figure 1.2**). Despite frequent inspections, the flooding resulted in unanticipated scouring around the bridge's piers, which, according to authorities, were the only ones in the municipality to not be built directly into underlying bedrock. The area surrounding the bridge was closed off to traffic and evacuated in order to ensure public safety (CTV News, 2013).

Figure 1.2. Derailed train in scour-related bridge collapse in Alberta (CTV News, 2013)

Scour refers to the removal of sediment in a natural flow system, which occurs due to a change in flow velocity. Depending on the cause of this change, scour can be characterized as one of two types: general or localised. General scour is the transport of channel bed material which would occur regardless of the presence of a bridge, due to seasonal or environmental changes in flow velocity, or changes in channel or geological characteristics (including the introduction of other hydraulic structures into the flow environment).

Localised scour refers to scour caused by the combined effects of contraction scour and local scour. The causation of contraction scour is the narrowing of a channel width where the bridge is introduced, resulting in a higher-velocity flow. Finally, local scour is caused by the presence of bridge piers and abutments in the flow. When these structures are introduced into a flow environment, they represent a disturbance in the flow; this disturbance results in an increase in transport of local sediment, causing scour holes to develop. Localised scour can be further characterized as either live-bed (where sediment transport exists) or clear-water scour (where bed material is at rest).

Although scour research has become quite extensive, scour-related failures still occur, which can be attributed to a lack of knowledge with respect to the process of scour, dated design criteria, and lack of publically available results from such research (Sumer and Fredsoe, 2002).

As previously discussed, with 60 percent of an average of 50 to 60 bridge failures per year in the United States occurring as a result of scour, scour holes play a significant role in bridge failure. Hence, scour is not only a safety concern, but an economical issue as well (Ettema et al., 1998). Bridge failure results in unexpected expenses, such as

provision of temporary transportation solutions (as described above in the case of the Calgary flooding collapse). These expenses have been shown to exceed what would have been the cost of replacing the bridge's damaged structural components and its road approaches altogether (Melville and Coleman, 2000).

As a result of its prevalence as a cause of bridge failure, scour is highly prioritized by modern bridge engineers. Several national and provincial bridge design codes (including the AASHTO LRFD, OHBDC, and CHBDC) include provisions for hydraulic design. Such provisions include recommendations for design of bridge piers with respect to scouring, which state that this design is to be done on the basis of one of several code-specified "approved methods." These methods refer to empirical equations which have been derived using experimental and field data over the past half-century. These equations are used to calculate the depth under which foundations must be placed in order to avoid failure due to scour. However, these widely used equations have a tendency to over-predict this depth (referred to as equilibrium scour depth, or d_{se}). While present understanding has improved and many scour depth prediction formulae are available (summarised in **Section 2.3**), these methods often yield vastly different results, suggesting that many aspects of scour are still not well understood.

While over-prediction is less problematic for small piers, when comparatively wider piers are placed at unnecessary depths, construction and material costs can far exceed what would be required with the use of a more accurate predictive method (Ettema et al., 1998). The variables which contribute to scour are many and varied, further complicating scour prediction. These factors include those relating to geomorphology of the channel itself, flow transport, bed sediment, and geometry of the

bridge in question (Melville and Coleman, 2000); while the complexity of the scouring process and varied nature of such contributing parameters are undoubtedly partially responsible for such an inclination, a phenomenon known as the scale effect is also a principal factor to which over-estimation of scour can be attributed.

In hydraulic modelling, scale effects refer to an imbalance of force ratios between model (laboratory) and prototype (field). If perfect geometric, kinematic, and dynamic similarity between model and prototype are not maintained, then scale effects will occur; however, the magnitude of these effects and their negligibility is highly dependent on the nature of the model in question (Heller, 2011).

In scour modelling, the principal difficulty in scaling lies in sediment size. This is demonstrated through the use of a scale factor, λ, which is the ratio of some characteristic length or dimension in the prototype to that same length or dimension in the model. While fluid and pier properties (such as water depth and pier diameter) can be scaled between field and laboratory with relative ease, the same cannot be said for sediment or bed material properties (Heller, 2011).

Sediment in a typical alluvial bed for which scour is a concern generally has a median sediment diameter in the range of 0.1 to 10 millimetres. If this median sediment size, or d_{50}, were held to the same scale factor as that of fluid and pier properties, its scaled counterpart in the model would be of such a size that the inter-particle forces between individual grains would be drastically altered; in effect, the sediment would behave cohesively. This would no longer accurately replicate flow-sediment interactions in the field, rendering the model itself inaccurate (Ettema et al., 1998).

As a result, in practice, d_{50} is held constant between the field and the prototype. While this solves the issue of sediment cohesiveness, it also compromises similarity, which results in scale effects. This manifests itself in the form of inaccurately deep scour in the model, and since results from such experimentation have been used to derive empirical equations for predicting scour, therefore demonstrates the relationship between scale effects and over-design of bridge pier scour depth in practice (Ettema et al., 1998).

1.2. Objectives

This research will further investigate scale effects on design estimation of scour depths at bridge piers. Relationships between various non-dimensional quantities in scour investigations will be explored. The objectives of this thesis are:

- To evaluate commonly-used bridge pier scour depth prediction methods using experimental data from previous investigations (including those from the University of Windsor)
- To experimentally explore scale effects in scour modelling by completing two phases of tests which isolate the influences of relative sediment size (D/d_{50}) and flow shallowness (h/D)
- To collectively analyze experimental results in scour modelling at the University of Windsor and subsequently develop a new scour depth estimation method based on said results

1.3. Scope of Work

A total of 22 experiments were carried out in the Sedimentation and Scour Study Laboratory at the University of Windsor's Ed Lumley Centre for Engineering Innovation. Experiments were performed in two different types of sand beds with 12 cylinder sizes.

CHAPTER 2

LITERATURE REVIEW

The literature review consists of an overview of the scouring process and its mechanisms as a cause of bridge failure, a description of the parameters affecting scour and their influence on equilibrium scour depth (determined through prior experimentation), an examination of bridge pier scour depth estimation methods, an explanation of scale effects in scour modelling, and design recommendations for scour (including scour mitigation techniques).

2.1. General Remarks

2.1.1. The Scouring Process

Flow around a bridge pier is a class of junction flow, or "flow [which develops] at the junction of a structural form and a base plane" (Ettema et al., 2011). The flow field around a pier consists of a horseshoe vortex system, wake or lee vortices, trailing vortices, or a combination of any of these (Chiew, 1984). This flow field is three-dimensional and unsteady due to the ongoing interactions between these turbulent flow structures (Ettema et al., 2011), which are illustrated in **Figure 2.1**.

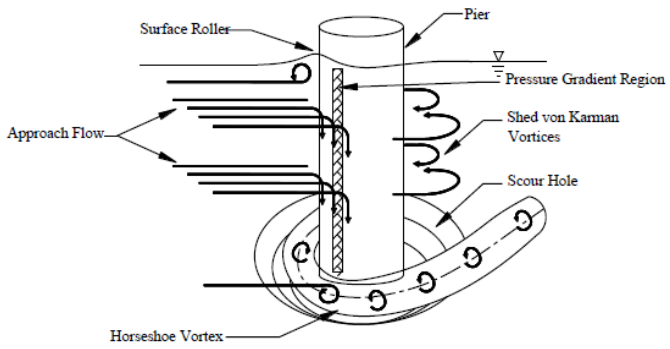

Figure 2.1. Depiction of flow structures in flow field around a pier (Hodi, 2009)

The magnitude of approach flow velocity (**Figure 2.1**) decreases in the vertical direction, such that maximum velocity occurs at the water surface and velocity at the channel bed is zero due to the no-slip condition. When the flow encounters the upstream face of the pier, velocity of flow abruptly becomes zero, and velocity at the sides of the pier increases. This causes pressure to decrease around the pier in the downstream direction (Figliola and Beasley, 2011). It is at this point (the pier sides) that scouring action will be initiated. Scour then increases in the upstream direction until the upstream face of the pier is reached, creating a partial "ring" of scoured material (Guo, 2012).

A downward pressure gradient will also form at the pier face, causing increased flow velocity in a downward motion (Dey et al., 1995). The downflow, once initiated, induces scouring action upstream of the pier (Chiew, 1984). The downflow will then curl up and around itself and the pier, initiating formation of the horseshoe vortex, which is named for its plan-view shape (Melville and Coleman, 2000). The aforementioned ring from the scoured sides of the pier then "traps" the still-forming horseshoe vortex, allowing rapid removal of sediment to commence and continue until equilibrium is reached (Guo, 2012).

For clear-water scour, the equilibrium scour state is defined by the point in time at which the velocity of flow circulation in the scour hole is no longer capable of removing bed material from the hole (Chiew, 1984), or when the shear stress caused by the horseshoe vortex is equal to the critical shear stress of the bed material at the bottom of the scour hole (Deng and Cai, 2010). The corresponding equilibrium scour depth represents, for live-bed scour, the scour depth at the point in the scour process at which the rate of sediment transport into the scour hole is equal to the rate of sediment transport

out of the scour hole (Chiew, 1984). In practice, equilibrium scour depth (d_{se}) can require many hours or even weeks to develop under clear-water conditions, and even when d_{se} is eventually reached, some removal and deposition of sediment may still occur in the vicinity of the scour hole; however, this continued scouring action is typically not significant enough to affect the "overall scour form" (Ettema et al., 2011).

As described, there are other turbulent structures in the flow field surrounding the pier which will affect scour. Wake vortices occur as a result of flow around a pier and the "surface roller" flow structure forms at the air-water interface (**Figure 2.1**). The behaviour of wake vortices mimics that of a tornado, removing sediment from the channel bed in an upward motion. The volume of sediment transported by wake vortices is smaller than the volume of sediment transported by the horseshoe vortex system. Trailing vortices are only induced in the case of a pier that is entirely submerged in the flow (Chiew, 1984), and extend from the top of the pier in a downstream direction (Breusers et al., 1977).

Once equilibrium has been attained, the scour hole is generally of an inverted-frustum shape; physically, the upstream slope of the hole tends to be close to the angle of repose of the sand in which it has formed (Ettema et al., 2011).

2.1.2. Scour as a Failure Mode

A structure (in this case, bridge) can be in danger of failure if one of its structural components (here, a pier or abutment) fails; pier and abutment foundations are therefore crucial in bridge stability, since failure of foundation is highly likely to result in the failure of the column it is supporting. It is necessary to recognize the ways in which a pier can fail such that the span it is supporting also fails or collapses.

If pier failure is considered primary failure, the pier foundation or foundation material has failed, and the pier will experience downward motion. The linkage or connection to the span (and therefore supporting action of the pier) then no longer exists or is compromised, and the span is therefore susceptible to failure and likely to collapse.

If the pier failure is considered secondary, the failure has resulted from motion of the pier in a vertical, lateral, or rotational direction. For example, lateral and vertical movement of the pier can occur as a result of seismic forces, and lateral and rotational pier motion occurs as a result of debris, ice, and marine traffic colliding with the pier. Vertical and rotational pier movement can occur due to scouring around the pier foundation and soil-bearing failure when scour reaches the foundation support (Lebeau and Wadia-Fascetti, 2007). In general, "piers fail as scour develops" (Ettema et al., 2011).

If equilibrium scour depth is not reached until after the pier or abutment foundations have been exposed, or in extreme cases, undermined, then failure of the foundation is likely to occur, resulting in failure of the pier and subsequent failure of the bridge itself. Pier structure (or pier type) will also affect the way in which a pier fails. Behaviour of piers with footings will differ from behaviour of piles during development of scour (Ettema et al., 2011).

2.2. Parameters Affecting Scour

2.2.1. Overview

Prediction of equilibrium scour depth can be done through the use of experimentally-derived empirical equations or computational methods. Temporal scour depth (time development of scour) can also be predicted using either of these methods.

Researchers have developed many formulae for predicting scour depth, the majority of which employ dissimilar combinations of variables to generate an estimated value of d_{se}/D, or relative scour depth (Deng and Cai, 2010).

The majority of variables which affect scour depth and geometry can be categorized into one of five groups, which are generally interdependent (Chiew, 1984):

- **fluid** properties (density, ρ; kinematic viscosity, ν; and temperature, which is not a primary concern in the lab but rather in the field, where it cannot be controlled)
- **time**, as scour is a temporal process, is also related to the type of scour under consideration (live-bed equilibrium is typically achieved within a shorter time period than in clear-water conditions); in the case of increased scour induced by flooding after a storm of some magnitude, the length of time of flooding or storm is pertinent
- **flow** properties (water depth, h; energy slope; shear stress in uniform flow; angle of attack, Θ; mean flow velocity, U; and critical velocity of bed material, U_c),
- **pier** characteristics (pier diameter, D; shape, Sh; surface condition; pier orientation; and debris accumulation)
- **sediment** characteristics (sediment density, ρ_s; median sediment size or diameter, d_{50}; uniformity of particle size distribution, σ_g; cohesiveness; shape factor; angle of repose; and fall velocity)

The parameters listed above can be further reduced to a set on which d_{se} has been found to rely most heavily. The majority of the formulae normally calculate equilibrium scour depth as a function of the parameters listed below (**Equation 2.1**):

$$d_{se} = f\{\rho, \nu, U, U_c, h, \rho_s, d_{50}, \sigma_g, g, D, Sh, Al\} \qquad \textbf{[2.1]}$$

As denoted by **Equation 2.1**, pier shape will also alter scour geometry and depth; a more streamlined pier will induce a weaker horseshoe vortex system, lessening intensity of scouring action. The scour depth of a square-nosed pier can be 1.2 times higher than the scour depth of a sharp-nosed pier, and 1.1 times the depth of scour for a cylindrical or otherwise blunt-nosed pier (Richardson et al., 1990).

Equation 2.1 can be further reduced to a set of non-dimensional parameters; this is contingent on maintenance of constant pier shape, flow alignment, high Reynolds number and subcritical Froude number (**Equation 2.2**):

$$\frac{d_{se}}{D} = f\left\{\frac{U}{U_c}, \frac{h}{D}, \frac{D}{d_{50}}\right\} \quad \textbf{[2.2]}$$

Experimentation has contributed to determination of the effect of each of these variables on scour depth and geometry, particularly in clear-water scour. Clear-water scour experimentation was more common than live-bed until the 1980s, when a sudden influx of results demonstrated that scour depth in live-bed conditions could exceed scour in clear-water conditions (Melville and Sutherland, 1988).

There are other scour-influencing factors which are difficult to quantify; for example, inter-particle behaviour in any given sediment will affect scour depth and development. Similarly, the propensity of sediment to develop bed formations (planar beds, ripples, dunes and anti-dunes) under certain flow conditions will also alter the magnitude of scour (Richardson et al., 1990). Additional parameters which are similarly difficult to quantify are discussed in **Section 2.2.6**.

2.2.2. *Sediment Influences and Sediment-Structure Interaction Influences*

2.2.2.1.Relative Sediment Size or Relative Coarseness, D/d_{50}

Perhaps the most influential parameter relating to sediment size is the ratio of pier diameter to median sediment grain size. The relationship between D/d_{50} (also known as relative sediment size or relative coarseness) and relative scour depth (d_{se}/D) has inconsistencies. It has been shown that relative scour depth is lesser when D/d_{50} is greater than 50 (**Figure 2.2**). However, relative scour depth has been shown to fluctuate with very large values of D/d_{50}, for reasons which are unclear. One of the greatest challenges in scour modelling lies in the inability of a model to accurately represent a field value of D/d_{50}, which will be discussed further (**Section 2.4**). As a result, it is very difficult to glean a distinct relationship between field-level values of relative coarseness and relative scour depth (Lee and Sturm, 2009).

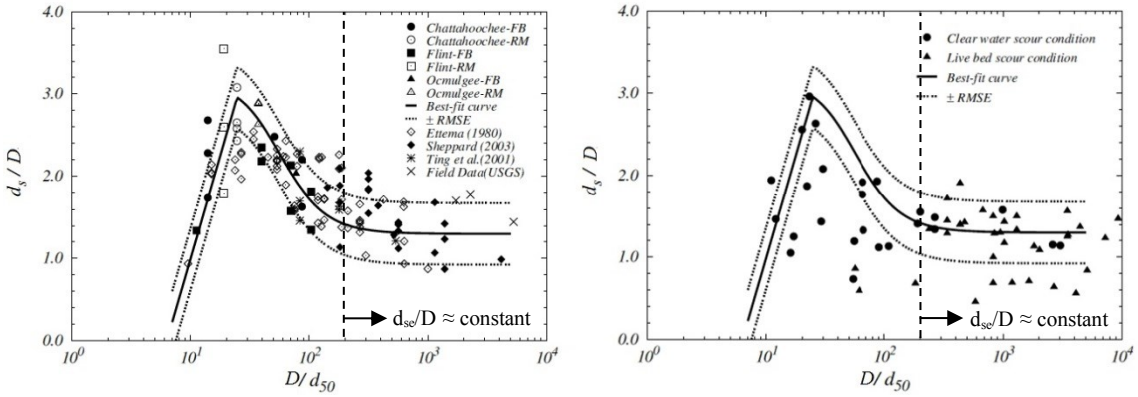

Figure 2.2. Graphical relationship between d_{se}/D and D/d_{50} (Lee and Sturm, 2009: used with permission from ASCE)

2.2.2.2.Sediment Type

As discussed above, sediment size does have an effect on scour for $D/d_{50} < 200$; however, d_{se} has also been shown to differ with sediment type. The majority of bridge pier scour experimentation focuses on flow systems with alluvial sand beds. Scour using

gravel as bed material has been investigated, with a d_{50} of 3.25 millimetres, for various pier shapes; the scour rate in gravel was found to be slower around a square cylinder. In addition, scour hole slopes were steeper around a square-shaped pier than for a circular pier. It was also observed that, even for gravel, scouring action began at the sides of a circular cylinder and reached the upstream face of the pier at approximately 1 to 2 percent of total time (Diab et al., 2010).

2.2.2.3.Sediment Cohesion

The effects of clay content, water content, bed shear strength, and pier Froude number on scour have also been investigated. It has been indicated that maximum equilibrium scour depth is similar in channel beds composed solely of clay or sand. However, in mixed-medium beds, a higher percentage of clay results in a lower value of scour depth. Specifically, scour depth decreased with an increase in clay content in a bed with a clay-sand mixture, when the bed also had a water content less than 24 percent. Scour depth decreased as clay content in the clay-sand bed increased up to 50 to 70 percent, after which scour depth increased for a mixed-medium bed with a water content greater than 27 percent (Debnath and Chaudhuri, 2010). For the purposes of this investigation, cohesive materials will not be used.

2.2.3. *Flow-Structure and Flow-Sediment Interaction Influences*

2.2.3.1.Flow Shallowness or Flow Field Scale, h/D

Variables do not affect scour depth solely on an individual basis. Several variables act collectively to influence scour. In this section, the ratio of h/D is discussed. Relative flow depth or flow shallowness (h/D) allows experimental or field bridge piers to be classified as narrow, wide, or intermediate. Narrow piers are the most commonly

studied class in research, for which h/D is greater than 1.4. For narrow piers, the greatest scour depth (i.e. the dimension with which researchers are primarily concerned) occurs at the upstream face of the pier. Wide piers are those whose h/D value is less than 0.2; for this class of piers, d_{se} is at a maximum near the pier flanks. Finally, intermediate piers are those whose h/D values fall between 0.2 and 1.4. In this range of transition, there is a further distinction which can be made; when h/D is approximately less than or equal to one, sediment deposits begin to affect scour hole development (Ettema et al., 2011).

Many scour estimation methods (discussed further in **Section 2.3**) include "K-values," or factors which account for various parameter influences. Melville's proposed K-value for flow shallowness was intended for an h/D value of 2.6, yielding unnecessarily high estimates of scour depth for wide piers in shallow flows. This was demonstrated in the case of two bridges in Maryland, United States, where relative flow depths were between 0.18 and 1.88, or smaller than Melville's assumed value of 2.6. In addition, while most scour prediction formulae require that the Froude number of flow be less than one, in shallow flows with wide bridge piers, the value of Froude number is much smaller than this (typically less than 0.2) (Johnson and Torrico, 1994).

Johnson and Torrico (1994) stated that relative scour depth (d_{se}/D) increased with relative flow depth at a decreasing rate, up until a limiting relative flow depth (typically at a relative flow depth of 2.6). After this point, h/D was not important but pier size in itself had a higher impact on scour depth. During experimentation, it is critical that all other variables that could have an effect on scour depth be held constant, such as flow velocity and bed material characteristics. In clear-water scour, the effects of flow shallowness with respect to relative sediment size have been previously shown to affect

development of local scour (shallow flow depths were shown to have no effect when D/d_{50} was very high, but flow shallowness did affect scour depth when D/d_{50} was low).

In effect, as flow depth increased, its influence on scour depth decreased, and the influence of pier size on scour depth increased, until a limiting point at which these influences reversed (Ettema et al., 2011). The results of this experimentation yielded a new K-value for wide piers in shallow flows, with the intention of predicting more reasonable estimates for scour depths at lower values of relative flow depth (Johnson and Torrico, 1994).

More recently, the influences of h/D on d_{se}/D can be defined by the classes of wide, narrow, and intermediate piers. As shown in **Figure 2.3**, the influence of h/D on d_{se}/D is greatest for wide piers, while for the class of narrow piers, there is very little influence of h/D on relative scour depth (Ettema et al., 2011).

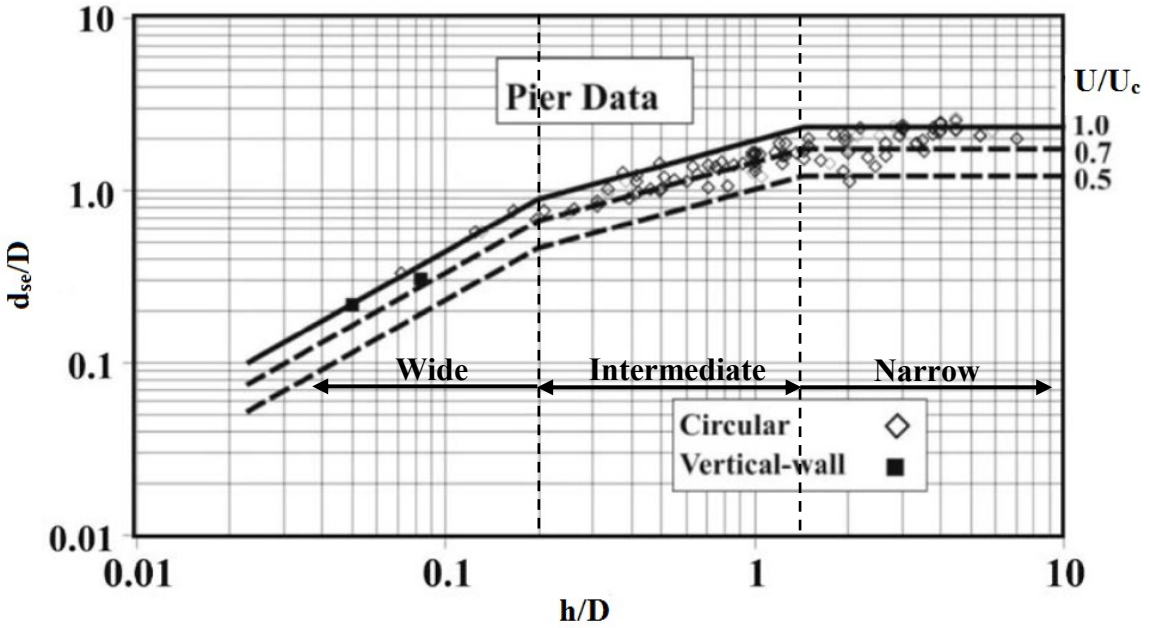

Figure 2.3. Graphical relationship between d_{se}/D and h/D based on U/U_c (Melville and Coleman, 2000: used with permission from Water Resources Publications)

Critical velocity of sediment (U_c) is the flow velocity at which incipient motion of sediment will occur, and must be determined for each sediment type under consideration. If flow velocity U exceeds U_c ($U/U_c > 1$), then sediment will be transported by the flow and live-bed scouring action will occur; if U/U_c is held below unity, then clear-water conditions will be maintained, which is typical of flow over alluvial sand beds. In **Figure 2.3**, it is clear that the effect of U/U_c is subdued compared to the influences of flow shallowness (h/D).

2.2.4. *Pier Influences*

2.2.4.1.Pier Diameter

Pier size is a governing parameter with one of the greatest influences on scour depth and geometry. Frequency of vortex shedding and the amount of vorticity in the wake of a pier are directly related to the projected width of a pier, demonstrating how influential D is on the surrounding flow field. Because of this, non-dimensional quantities are typically compared with d_{se} normalized with pier diameter (i.e. h/D and D/d_{50}, etc. are plotted with d_{se}/D) in order to isolate the effects of these variables without influence from pier diameter alone (Ettema et al., 2006).

If all test parameters are held constant and pier diameter D is increased, the frequency of vortex shedding will decrease, causing a subsequent decrease in d_{se}/D; similarly, as pier diameter is increased, D/d_{50} will increase and d_{se}/D will decrease, demonstrating the relationship between relative sediment size and frequency of vortex shedding (Ettema et al., 2006).

2.2.4.2.Blockage Ratio, D/b

The effects of blockage of a flow channel have been extensively investigated at the University of Windsor by Hodi (2009), D'Alessandro (2013), and Tejada (2014). It has been previously stated in literature that the blockage effects are negligible if blockage ratio (D/b) is held below ten percent (Chiew, 1984). However, previous experimentation had been shown to employ testing conditions for which blockage ratio exceeded this recommended value; since data from these experiments would have been used for development of empirical equations for pier design, use of this equations might not have been judicious.

It has since been determined that scour depth is greater in tests with smaller flume widths and higher blockage ratios, and that there are changes to d_{se} even when very small changes in D/b are applied (between 2.2 percent and five percent). As blockage ratio increased, there were greater discrepancies in both scour depth and geometry (Hodi, 2009). This was also confirmed for small values of D/d_{50} (D'Alessandro, 2013). However, when compared with tests performed for larger values of D/d_{50}, the influences of blockage ratio on d_{se}/D when $D/d_{50} < 100$ were shown to be "minimal" (Tejada, 2014).

2.2.4.3.Pier Configuration

The mechanisms by which bridge pier configuration alters scour geometry have also been investigated. During the design process, bridge piers are typically treated as isolated and effects of proximity are ignored; however, scour geometry has been shown to experience a change as a result of mutual interference of flow fields around closely-spaced piers. Thus, treatment of piers as isolated during the design process can lead to bridge failure. This investigation showed that when the centerline pier spacing between

piers was zero, the scour depth was 95 percent higher than that of an isolated pier of diameter D under the same conditions. When pier spacing was equal to D, the scour depth was still relatively larger by a factor of 1.21. As the ratio of spacing to D increased, scour depth continued to decrease from this point, until spacing was 8D, at which point the scour depth had approached that of an isolated pier (Beg, 2010).

2.2.5. *Time Development of Scour*

2.2.5.1.Unsteady Flow

Unsteady flow in natural flow systems poses a unique scouring situation. Varying flow may not only affect scour geometry, but time development of scour as well. The effects of varying flow on temporal scour were investigated by Lai et al. (2009), and were quantified using the flood or flow hydrograph. An unsteady flow factor was derived using peak-flow intensity and time-to-peak of the hydrograph, and then utilized in a relation to estimate d_{se} for uniform bed material conditions.

When using empirical equations to estimate scour depth, the flow depth and velocity quantities correspond to peak flow conditions. In order to estimate scour depths under unsteady flow conditions, tests were performed for two types of flow (steady flow, and linearly rising followed by steady flow). The length and nature of the rising portion of the hydrograph was shown to affect scour, and relations for predicting scour under unsteady flow conditions were derived (Lai et al., 2009).

2.2.6. *Other Parameters*

As discussed in **Section 2.2.1.**, there are several conditions which exist at bridge pier sites which are difficult to quantify. Among these characteristics is pier length, which does not affect scour depth unless the pier is at an angle to the flow, in which case

the scour depth can be 1.33 times greater for a pier twice as long as its diameter if it were a cylindrical pier. This also emphasizes the importance of angle of attack on scour depth (Richardson et al., 1990).

The nature of the channel itself can also have an effect on scour depth; for example, if a bridge is located in close proximity to a bend in the flow channel, oncoming flow will increase in magnitude and scour may be enhanced. Rainfall and floodplain behaviour can also alter scouring action; if flooding is to be expected on a seasonal basis, scour can become cyclic in nature (Richardson et al., 1990).

Flow systems in which ice is formed and debris is prominent will modify scour depth; when ice and debris such as tree branches and litter are caught around bridge piers, this effectively increases the pier width, subsequently increasing scour (Richardson et al., 1990).

2.3. Scour Depth Estimation Methods

2.3.1. Overview

Despite the wide and varied nature of scour-affecting parameters, many researchers have found that scour depth can be defined by three quantities:

1. Flow intensity (upstream depth-averaged velocity divided by critical depth-averaged velocity of sediment), U/U_c
2. Relative flow depth or flow shallowness (water depth divided by pier diameter or width), h/D
3. Relative sediment size or relative coarseness (pier diameter divided by median sediment grain size), D/d_{50} (principal differentiating factor between laboratory and field)

Empirical equations that were developed comparatively early on in bridge pier scour research attempted to predict equilibrium scour depth using the various permutations of similar variables. They have been mainly been developed for systems under clear-water conditions with non-cohesive sediments (Guo, 2012).

This literature review and subsequent analysis will focus on five predictive methods, which have been developed over the past half-century. The equations were selected on the basis of commonality of use in practice, practicality or applicability to considered results in analysis, and relative recentness of development.

2.3.2. Jain's Equation (1981)

Jain's equation was derived though analysis of available experimental data. This investigation noted that there was a large amount of scatter in the available data, and that it was difficult to determine any meaningful relationships or curves between d_{se}/D and other parameters at particularly high and low values of Fr and h/D. Jain also stated that, at the time of publication, previously-developed scour estimation equations were only applicable under the "same conditions in which they were derived." The equation that was eventually derived from this analysis calculates relative scour depth as a function of h/D and critical Froude number, Fr_c:

$$\frac{d_{se}}{D} = 1.84 \left(\frac{h}{D}\right)^{0.3} Fr_c{}^{0.25} \qquad \textbf{[2.3]}$$

2.3.3. Melville and Sutherland Equation (1988)

The Melville and Sutherland equation was developed based on envelope curves drawn to fit laboratory data. The equation is based on a maximum estimation of d_{se}/D, which has conventionally been accepted as 2.4; this maximum value is then reduced

through a series of "K" parameters, which are each intended to account for a specific condition in the scouring process:

$$\frac{d_{se}}{D} = K_1 K_y K_d K_\sigma K_s K_\alpha \qquad \textbf{[2.4]}$$

where, K_1 is a flow intensity parameter, K_y is a flow depth parameter, K_d is a sediment size parameter, K_σ is a sediment gradation parameter, K_s is a pier shape parameter and K_α is a pier alignment parameter. The Melville and Sutherland equation takes the form of a design method, following a series of calculations, derivations, and extrapolation steps, each of which yields a separate K value, allowing for final calculation of d_{se}/D.

2.3.4. Froehlich Equation (1988)

Unlike many of its predecessors, the Froehlich equation was developed through the use of field data. Regression of over 70 field data points was employed in order to develop a predictive formula which accounted for pier shape and approach flow angle of attack (where a* is the effective pier diameter and φ is a pier nose shape factor):

$$\frac{d_{se}}{D} = 0.32\varphi F_r^{0.2}\left(\frac{a^*}{D}\right)^{0.62}\left(\frac{h}{D}\right)^{0.46}\left(\frac{D}{d_{50}}\right)^{0.08} + 1 \qquad \textbf{[2.5]}$$

2.3.5. HEC-18 or Colorado State University Equation (2001)

The most commonly used equation for prediction of equilibrium scour depth is the HEC-18 or CSU equation, which was published by the Hydraulic Engineering Circular No. 18 in 1993. The HEC-18 equation, also known as the CSU equation, also uses "K" correction factors and can be used for clear-water and live-bed conditions (Deng and Cai, 2010).

The first version of the HEC-18 equation included three correction factors, which accounted for pier nose shape, angle of attack of approach flow, and bed condition,

respectively; a fourth K factor was added to the equation in 2001, and was intended to adjust d_{se}/D based on armoring conditions by bed material size:

$$\frac{d_{se}}{D} = 2.0K_1K_2K_3K_4\left(\frac{h}{D}\right)^{0.35}F_r^{0.43} \qquad \textbf{[2.6]}$$

2.3.6. Sheppard-Melville (S/M) Equation (2011, 2014)

The Sheppard-Melville or S/M equation (2011, 2014) approaches scour depth prediction through consideration of interactions between flow, structure, and sediment, in order to obtain the maximum potential scour depth:

$$\frac{d_{se}}{D} = 2.5f_1f_2f_3 \qquad \textbf{[2.7]}$$

where f_1 is representative of flow-structure interactions, f_2 accounts for flow-sediment interactions, and f_3 is indicative of sediment-structure interactions.

$$f_1 = \tanh\left[\left(\frac{h}{D}\right)^{0.4}\right] \qquad \textbf{[2.7a]}$$

$$f_2 = \left\{1 - 1.2\left[\ln\left(\frac{U}{U_c}\right)\right]^2\right\} \qquad \textbf{[2.7b]}$$

$$f_3 = \left[\frac{\left(\frac{a^*}{D_{50}}\right)}{0.4\left(\frac{a^*}{D_{50}}\right)^{1.2} + 10.6\left(\frac{a^*}{D_{50}}\right)^{-0.13}}\right] \qquad \textbf{[2.7c]}$$

2.3.7. Evaluation of Estimation Methods

While the majority of provisions in the United States utilize the HEC-18 or CSU equation for hydraulic design of bridge piers, recent developments in scour research have indicated the need for an updated equation (Ettema et al., 2011). Several investigations have served to compare these equations with experimental results and determine which of them, if any, offer an accurate prediction of bridge scour. Many have also compared such

predictions with field data for model-prototype accuracy. The HEC-18 equation appeared to rarely offer a low estimate of scour depth, but often generated an unnecessarily high prediction. For serviceability concerns, conservative estimates are clearly more desirable than low estimates; however, such estimation will yield an uneconomical design (Guo, 2012). As discussed, this over-estimation occurs as a result of various phenomena. One of these, which is a primary weakness of currently used equilibrium scour depth estimation methods, lies in their failure to include or articulate some pertinent influences (Ettema et al., 2011).

An evaluation of various estimation methods, including several of those detailed above (**Sections 2.3.2.** through **2.3.6.**) was carried out through graphical relations. Experimental data was compared with several predictive methods (**Figure 2.4**), in order to determine any limitations on their use. It was determined that the HEC-18 equation, Froehlich equation, Melville and Sutherland equation, and Sheppard-Melville equation all over-predicted d_{se}/D to varying degrees, except in cases where the investigations in question dealt with scale effects. For large-scale tests, the HEC-18 equation was the most accurate method of prediction. For tests with values of U^2/gD greater than 0.1, the Froehlich equation resulted in the lowest over-prediction; conversely, the same equation over-predicted d_{se}/D to the highest degree for values of U^2/gD less than one (Williams et al., 2013).

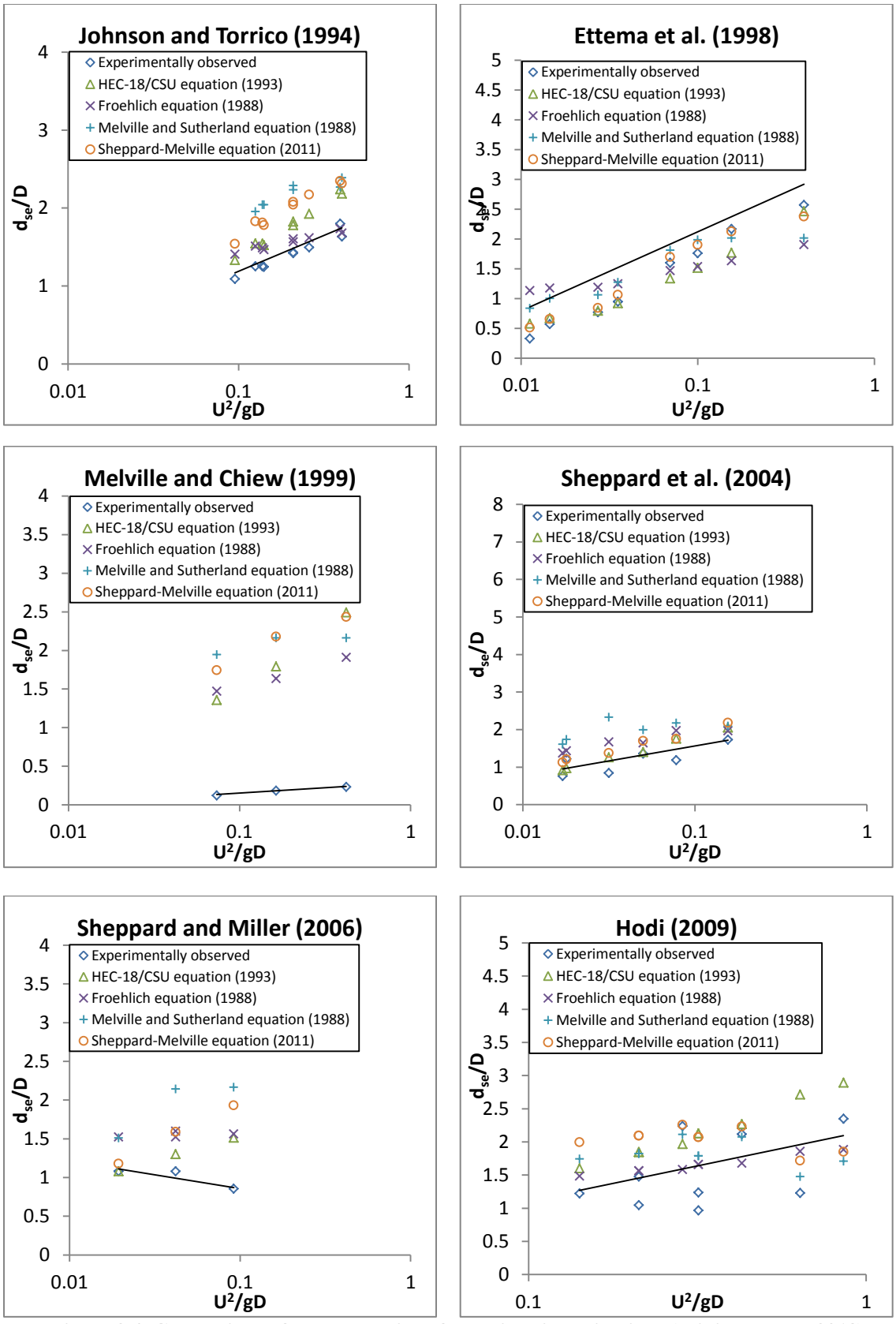

Figure 2.4. Comparison of scour equations for various investigations (Williams et al., 2013)

Early on in the quest for accurate scour prediction methods, it was evident that the aforementioned variety of parameters which contribute to scour geometry complicated prediction. The goal of many researchers was to develop a means of predicting scour in natural flow systems, with the hope of alleviating the high rates of bridge failure due to scour.

Field measurements were also taken to observe scale effects from the field to laboratory, with the bridge site in question chosen such that local scour, not contraction scour, was the main cause of bed degradation, and angle of attack of flow was in the same plane as the bridge pier. Accumulated debris was also found to have an adverse effect on scour depth; a suggestion for design was to include an "arrestor," or protection at the base of the pier, approximately the size of the predicted scour hole, in order to alleviate scour depth (Laursen and Toch, 1956).

Although the presented formulae provide an acceptable prediction of scour depth in the field, actual conditions in natural flow systems are not a consideration here; for example, clear-water scour in channels with uniform sediment is uncommon. The formation of armored beds in natural flow systems is an example of this lack of uniformity.

Taking into consideration these complexities, it is evident that use of a single formula is not an adequate means of predicting scour. It is suggested that local scour be estimated by multiple methods in order to arrive at the best possible estimate. Recommendations include dimensional analysis of the variables involved, consideration of the relationship of bed material transport (total transport into the hole – total transport

out of the hole = rate of transport), and regression analysis of available data (Sheppard et al., 2004).

While development of empirical equations for scour prediction is ongoing, another form of scour prediction is being investigated as well. The use of artificial neural networks (ANN) and computational fluid dynamics (CFD) has been initiated for the purposes of flow simulation and scour prediction. Raw data in the form of such parameters acts as the input layer of the network, and the ANN is "trained" to determine relationships between these parameters and produce an output layer. Examples of the input parameters that have been used for the input layer are flow depth, mean velocity, critical flow velocity, mean grain diameter, and pier diameter. As previously mentioned, the use of computational methods for scour prediction is still new and complicated by the intricacies of the scouring process; further investigation into this estimation method is required (Guo, 2012).

2.4. The Scale Effect

2.4.1. Scale Effects in Hydraulic Modelling

In modelling, scaling is defined by scale ratio or scale factor, λ, which is the ratio of some characteristic length or dimension in the prototype or field to that same length or dimension in the model or laboratory. In general, as λ increases, so do scale effects. Physical models such as those involved in hydraulic experimentation may avoid scale effects if geometric, kinematic, and dynamic similarity is observed between model and prototype. In scour modelling, inertial, gravitational, and viscous forces are of particular importance for similarity (Heller, 2011).

2.4.2. Scale Effects in Scour Modelling

In scour modelling, pier Reynolds number (Re) is typically high and resulting scale effects are taken as negligible. Therefore, Froude number constancy is considered most relevant and experimental design adheres to this form of similitude. Re has been shown to have little to no effect on scour depth as long as flow around the pier is fully turbulent (Heller, 2011).

The scale effect of laboratory to field results of scour depth has demonstrated that laboratory conditions yield deeper values of relative scour depth than will occur in natural flow systems. This indicates that experimentally-derived formulae generally over-predict scour depths. One of the main causes for this deviation is due to sediment size scaling (Ettema et al., 1998).

Scale effects in scour modelling occur due to the difficulty in simultaneously satisfying three length scales in scour models: h, D, and d_{50}. The similitude in energy and frequency of vortex shedding between model and prototype piers (previously discussed in **Section 1.1**) can be described by the non-dimensional quantities of pier Euler number ($Eu_d = U^2/gD$, where g is equal to gravitational acceleration) and pier Reynolds number ($Re = \rho UD/\mu = UD/\nu$). Eu_d is of particular use in relating energy gradients in the flow field surrounding a bridge pier; physically, it is it the ratio of stagnation head at the upstream face of the pier ($U^2/2g$) to pier width, D (Ettema et al., 2011).

As previously described, sediment size cannot truly be scaled in the same fashion as flow and pier characteristics. Adequately small sediment sizes that would achieve similar scaling exist in cohesive soils, whose behaviour would not accurately replicate that of the actual bed material in the field (Ettema et al., 1998). This scaling inaccuracy

results in a distorted ratio of pier width to sediment size, resulting in larger anticipated scour depths than will actually occur in the field. The geometric factor by which all other variables are scaled is not consistent for sediment size, generating overly conservative predictions (Lee and Sturm, 2009).

Larger sediment sizes in the laboratory can also affect other flow properties, propagating the scale effect beyond the noticeable variables. Froude number, Fr, has been shown to have an influence on magnitude of scour depth. In the case of flow around a bridge pier, the Froude number indicates the effect of the previously described pressure gradient around the circumference of the pier. A lower value of Fr results in a smaller scour depth. When sediment cannot be properly scaled and flow intensity (U/U_c) is maintained constant, Froude number similarity is affected (Lee and Sturm, 2009).

This inability to properly scale D/d_{50} also results in flow field dissimilarity; specifically, pressure heads along flow paths between models and prototype are scaled to the same degree as other physical quantities (D, h, etc.). Therefore, if d_{50} is not scaled similarly, then flow field similitude will also be altered (Ettema et al., 2011).

Consistency of laboratory conditions also contributes to the scale effect. Flow in an artificial flume is typically laminar, while conditions in the field are less consistent. Bed material sediment is purposely well-graded in the laboratory, which is not always the case in natural flow systems. Wall interference due to channel blockage is also an issue in scour modelling, but not a concern in the field. As described, computational fluid dynamics (CFD) are being used increasingly to replicate field flow conditions in the laboratory (Ettema et al., 1998).

Current d_{se} estimation methods typically fail to account for scaling of frequency and vorticity of large-scale turbulence structures, which also contributes to over-prediction and subsequent over-design of bridge piers. In 2006, Ettema et al. presented an investigation on two new parameters which were intended to describe scale effects and their influence on d_{se}: frequency of vortex shedding and amount of vorticity in the wake of a pier (Ettema et al., 2006).

2.5. Scour Mitigation and Recommended Design Considerations

Though not an objective of this study, there are measures which are used to partially protect piers against scouring action; for completion purposes, these measures will be discussed briefly in the following section. While "complete" protection against scour is not economically practical, there are two types of protection that are commonly used: armouring and flow alteration (Khwairakpam and Mazumdar, 2009).

Armouring can either occur naturally, or consist of placing an armouring layer (riprap, tetrapods, cable-tied blocks, grout-filled bags, mattresses, concrete aprons, etc.) at the surface of a channel bed or within an existing scour hole (Deng and Cai, 2010). Armoured beds or layers can develop naturally during times of peak or above-average flows; finer sediment is then washed away in areas of the channel bed, exposing coarser-grained sediment in formations known as armour beds or armour layers. Once the armour layer's critical velocity has been reached (i.e. the layer or bed has been breached), this higher velocity impinges upon the underlying fines, creating a greater scour depth than would have resulted without the armour bed. This phenomenon is avoided if a secondary armour layer exists. A design method has been derived to determine scour depth in cases where the channel bed has armouring (Raikar and Dey, 2009).

Flow alteration includes the use of splitter plates, submerged vanes, collars, slots and sacrificial piers to alter the flow field surrounding the pier. Collars, in particular, work to reduce downflow, therefore reducing the strength of the horseshoe vortex; its efficiency is dependent on its size and placement (Deng and Cai, 2010). Splitter plates are often used in tandem with riprap (armouring) and have been shown to reduce scour depths by up to 60 percent. Helical wires and cables are also used to alter the flow field around piers; wire or cable diameter, distance between threads, and threading angle all have an impact on the effectiveness of this curative measure. Despite the effectiveness of these measures, no "foolproof" scour protection or prevention has been determined (Khwairakpam and Mazumdar, 2009).

2.6. Scour in the Field

By graphing field values of scour with various non-dimensional parameters, it is possible to demonstrate scale effects between laboratory and field scour. **Figure 2.5** shows the graphical relationship between relative coarseness D/d_{50} and field values of relative scour depth, while **Figure 2.6** shows the same for the relationship of flow shallowness h/D for the same field values.

In **Figure 2.5**, all field values of scour are shown to fall under Lee and Sturm's (2009) mean curve (previously discussed in **Section 2.2.2.**). However, for very high values of D/d_{50} (greater than 1000), d_{se}/D appears to decrease. While it is obviously unreasonable for such high values of D/d_{50} to be attained in a typical laboratory without use of cohesive sediment, further investigation into field measurements is required in order to properly explore the influence of D/d_{50} on d_{se}/D at such a range of D/d_{50}.

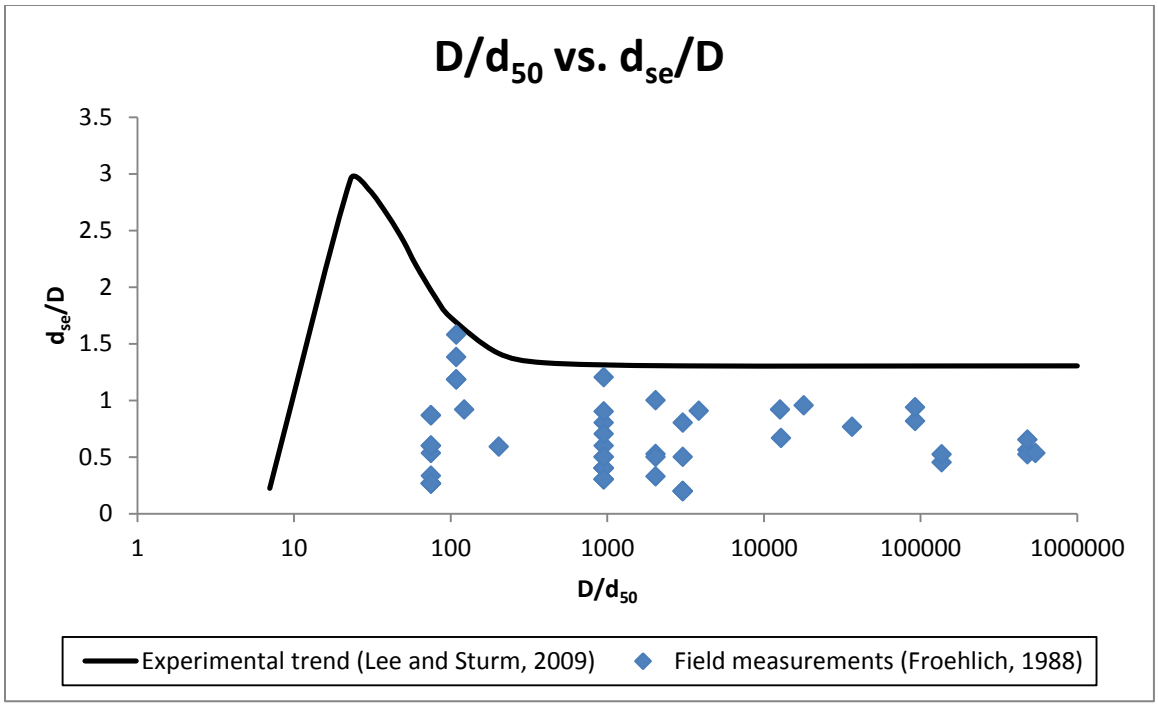

Figure 2.5. Graphical depiction of scale effects using field measurements of scour

In **Figure 2.6**, a trendline developed by Melville and Coleman (2000) is included for comparative purposes; this trend is indicative of the type of experimental results which have been used to derive scour prediction equations, and clearly demonstrates the discrepancies between field and laboratory measurements of scour. All field values presented by Froehlich in 1988 sit well below Melville and Coleman's (2000) trendline. Furthermore, Melville and Coleman's trendline indicates that after an h/D value of 1.4 has been reached, h/D no longer affects the magnitude of d_{se}/D; this is not confirmed by the field measurements and despite the low sample size of h/D values greater than 3, the field data indicates that d_{se}/D appears to decrease with increasing h/D after this value.

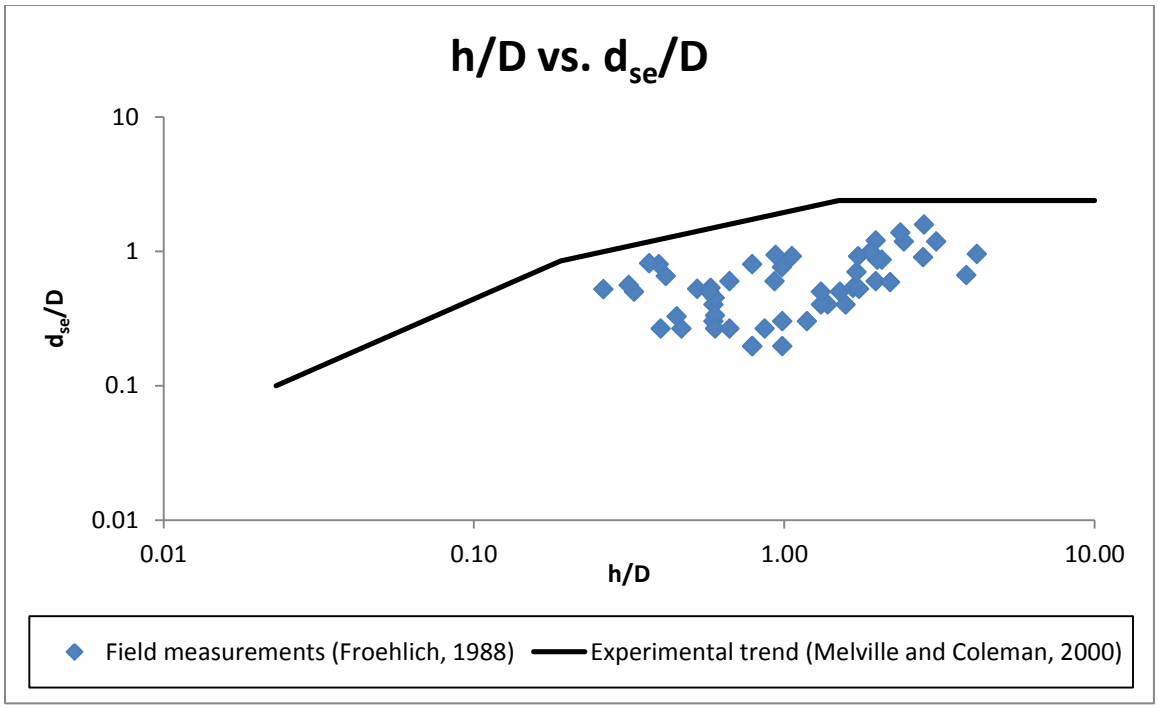

Figure 2.6. Graphical depiction of relationship between flow shallowness and relative scour depth based on field measurements of scour

CHAPTER 3

METHODOLOGY

3.1. Experimental Set-up

Experimentation was conducted in the Ed Lumley Centre for Engineering Innovation's Sedimentation and Scour Study Laboratory at the University of Windsor in Ontario, Canada. The experiments were conducted in a horizontal flume with a length of 10.5 m, a width of 1.22 m, and a height of 0.84 m. A flow straightener, constructed from layers of pipe (d = 0.5 in) and secured with silicone, was placed at the upstream end of the flume in order to regulate the flow. A plywood approach ramp was constructed in order to allow flow progression to a plywood box which held the required bed sediment. The pump flow controller was calibrated using a V-notch weir at the downstream end of the flume; the flume and pump have been used in other scour studies and flow quality has been ensured.

3.2. Bed Material

An ASTM sieve analysis was performed for two sands in order to determine the grain size distribution and relevant characteristics of each (**Figure 3.1**). The d_{50} values were found to be 0.51 mm for the "Fine 1" sand, and 0.77 mm for the "Fine 2" sand; the standard deviation of particle size ($\sigma_g = \sqrt{d_{84}/d_{16}}$) of each was 1.16 and 1.34, respectively. The sieve analyses indicated that the sediments were uniformly distributed.

For each sediment type, the critical velocity (U_c) was determined experimentally and analytically. After sediment had been loaded into the flume and levelled, the water depth was brought up to 12 cm and the pump was turned on. The pump frequency was increased incrementally until incipient motion of the sand particles was observed. The

given frequency was then related to a flow velocity using the previously-derived calibration curve; 85 percent of this velocity was used as the mean approach flow velocity for all tests in that particular sand. Critical velocity was found to be 0.263 m/s for the fine sand and 0.305 m/s for the coarse sand.

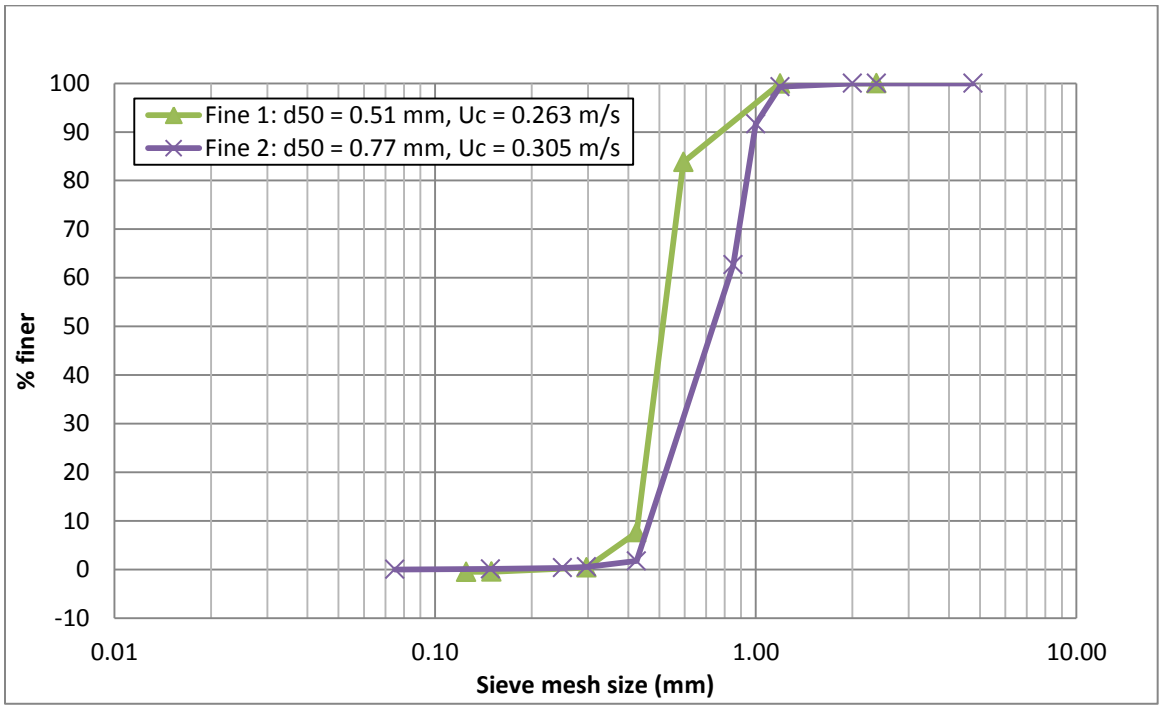

Figure 3.1. ASTM sieve analyses for bed sediment used in experimentation

3.3. Experimental Design

Experimentation was divided into two phases, each with two series of tests (shown in **Table 3.1**). Phase I consisted of twelve tests, with six tests conducted for d_{50} = 0.51 mm (series "A") and d_{50} = 0.77 mm (series "B"). For each test in phase 1, the blockage ratio (D/b = 10%), flow shallowness (h/D = 1.6), and flow intensity (U/U_c = 0.85) were held constant, such that the only varying non-dimensional parameter was relative coarseness. Flow shallowness was maintained above 1.4 in order to ensure that piers were classified as narrow (as per Melville and Coleman's (2000) trendline,

discussed in **Section 2.2.3**). The purpose of all phase I tests was to isolate the effects of D/d_{50} on relative scour depth.

In phase II, two series of tests ("E" and "F") were carried out in each sand bed in order to investigate the effects of flow shallowness (h/D) on scour geometry (e.g. d_{se}/D). These series consisted of 6 and 5 tests, respectively, in which the sole varying parameter was h/D.

Table 3.1: Experimental Work Plan

Test ID	D (m)	d_{50} (mm)	h (m)	b (m)	U (m/s)	Fr	U/U_c	D/b	h/D	D/d_{50}	b/h	Re
A1	0.121	0.51	0.193	1.22	0.224	0.162	0.85	0.1	1.6	237	6.31	2.7E+04
A2	0.101	0.51	0.161	1.02	0.224	0.178	0.85	0.1	1.6	198	6.31	2.3E+04
A3	0.089	0.51	0.142	0.90	0.224	0.189	0.85	0.1	1.6	174	6.31	2.0E+04
A4	0.079	0.51	0.127	0.80	0.224	0.200	0.85	0.1	1.6	156	6.31	1.8E+04
A5	0.070	0.51	0.112	0.71	0.224	0.213	0.85	0.1	1.6	137	6.31	1.6E+04
A6	0.060	0.51	0.096	0.61	0.224	0.230	0.85	0.1	1.6	118	6.31	1.3E+04
B1	0.121	0.77	0.193	1.22	0.259	0.188	0.85	0.1	1.6	157	6.31	3.1E+04
B2	0.101	0.77	0.161	1.02	0.259	0.206	0.85	0.1	1.6	131	6.31	2.6E+04
B3	0.089	0.77	0.142	0.90	0.259	0.219	0.85	0.1	1.6	115	6.31	2.3E+04
B4	0.079	0.77	0.127	0.80	0.259	0.232	0.85	0.1	1.6	103	6.31	2.1E+04
B5	0.070	0.77	0.112	0.71	0.259	0.247	0.85	0.1	1.6	91	6.31	1.8E+04
B6	0.060	0.77	0.096	0.61	0.259	0.266	0.85	0.1	1.6	78	6.31	1.6E+04
E1	0.060	0.51	0.240	0.61	0.224	0.146	0.85	0.1	4.0	118	2.54	1.3E+04
E2	0.060	0.51	0.192	0.61	0.224	0.163	0.85	0.1	3.2	118	3.17	1.3E+04
E3	0.060	0.51	0.144	0.61	0.224	0.188	0.85	0.1	2.4	118	4.23	1.3E+04
E4	0.060	0.51	0.120	0.61	0.224	0.206	0.85	0.1	2.0	118	5.08	1.3E+04
E5	0.060	0.51	0.112	0.61	0.224	0.213	0.85	0.1	1.9	118	5.43	1.3E+04
E6	0.060	0.51	0.085	0.61	0.224	0.245	0.85	0.1	1.4	118	7.16	1.3E+04
F1	0.060	0.77	0.241	0.61	0.259	0.168	0.85	0.1	4.0	78	2.51	1.6E+04
F2	0.060	0.77	0.193	0.61	0.259	0.188	0.85	0.1	3.2	78	3.14	1.6E+04
F3	0.060	0.77	0.142	0.61	0.259	0.217	0.85	0.1	2.4	78	4.19	1.6E+04
F4	0.060	0.77	0.120	0.61	0.259	0.239	0.85	0.1	2.0	78	5.05	1.6E+04
F5	0.060	0.77	0.096	0.61	0.259	0.266	0.85	0.1	1.6	78	6.31	1.6E+04

3.4. Experimental Procedure

Each experiment was carried out for 48 hours. It was determined through experimentation that there was a negligible difference in equilibrium depth of scour (d_{se}) in tests with run times of 72 hours and 48 hours. Therefore, 48 hours was deemed an acceptable length of testing time for the purposes of this investigation.

For each test series, the appropriate sand was placed in the sand box inside the flume. Following this, the walls were positioned in the sand bed such that the desired flume width was achieved. If flow depth (h) exceeded 20 cm for a particular test, the walls were replaced by those of a greater height and held in place using wooden braces (**Figures 3.2** and **3.3**). Once the walls were in place, the bed material was carefully levelled using a flat trowel and checked periodically with a bubble level to ensure a flat control surface.

Once the control surface was levelled, a model pier was centered between the walls. The pier was placed at a minimum of 1 meter downstream from the leading edge of the sand bed. Finally, the flume was filled to the desired water depth, the pump was turned on and brought up to a frequency necessary to sustain a flow intensity of 0.85. The depth-averaged velocity of the approach flow, U, was verified for each test using an Acoustic Doppler Velocimeter (ADV, Nortek USA); point measurements were taken at 0.2 and 0.8 of the total water depth and then averaged in order to determine U. This test was then left to run for 48 hours.

Once the 48-hour run time had elapsed, the pump frequency was gradually brought down and then shut off. The flume was then drained such that flow emptied in a downstream direction, in order to avoid displacement of bed material. Once the flume

was completely drained, the centreline and contour profiles of the scour hole were measured using a Leica laser distance meter mounted on a biaxial traverse.

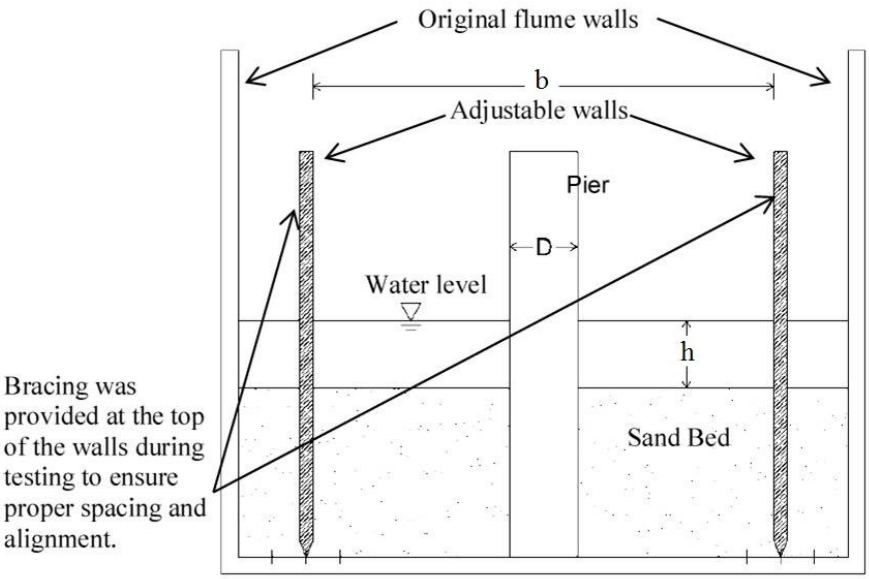

Figure 3.2. Schematic drawing of flume cross-section (D'Alessandro, 2013)

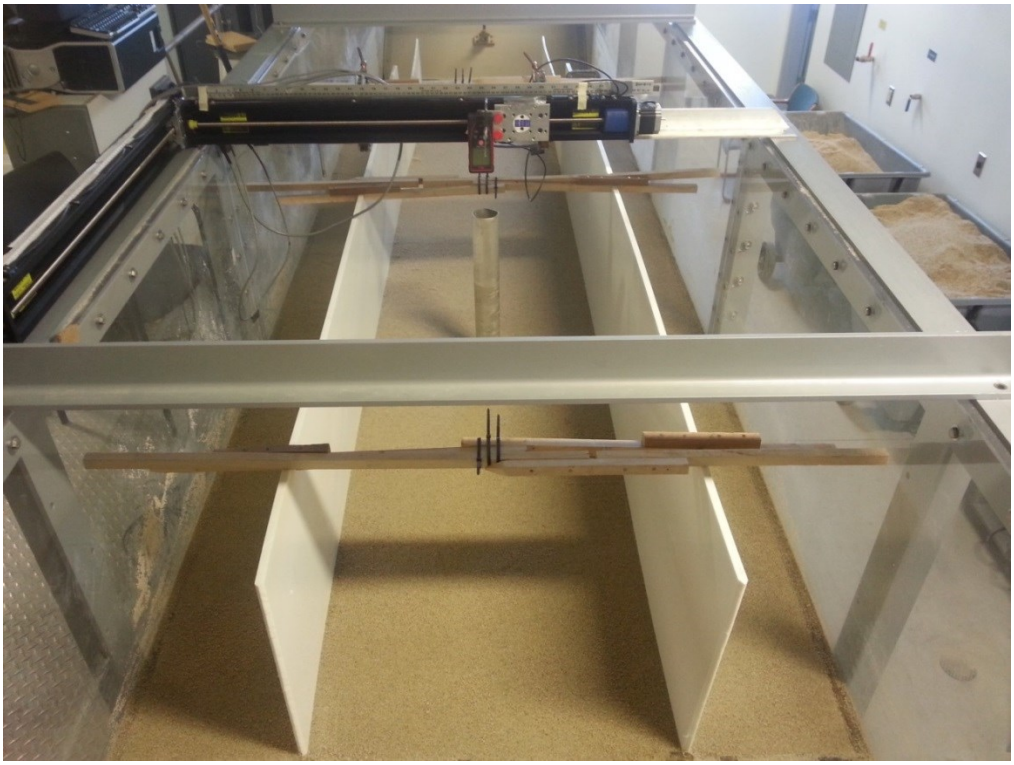

Figure 3.3. Experimental set-up

To obtain a centreline profile of scour, the laser was centred at the base of the pier. Point measurements were taken from the upstream edge of the scour hole until at least the point at which scour reached the walls downstream of the pier (**Figure 3.4**). The contour of the scour hole was traced while the flume was draining; once the water level was at the bed level, the contour was carefully marked around the outer edge of the water. The laser was then turned on and measurements were taken along half of the outline of the contour (**Figure 3.5**).

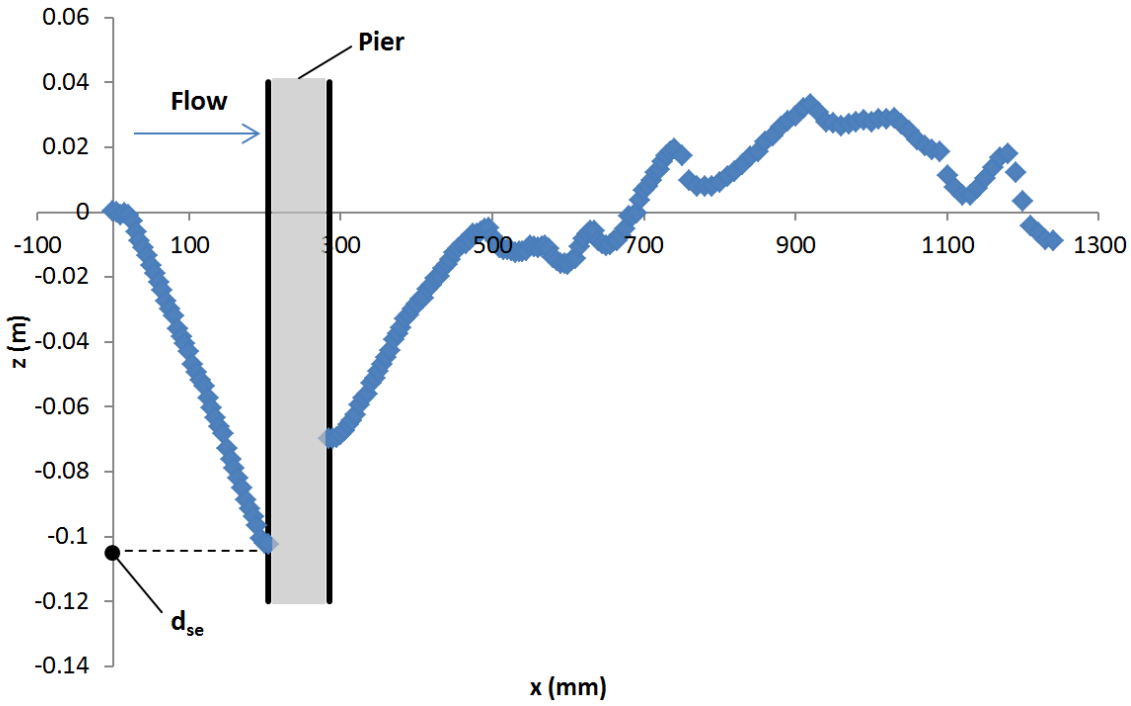

Figure 3.4. Point measurements of the centreline profile of a scour hole

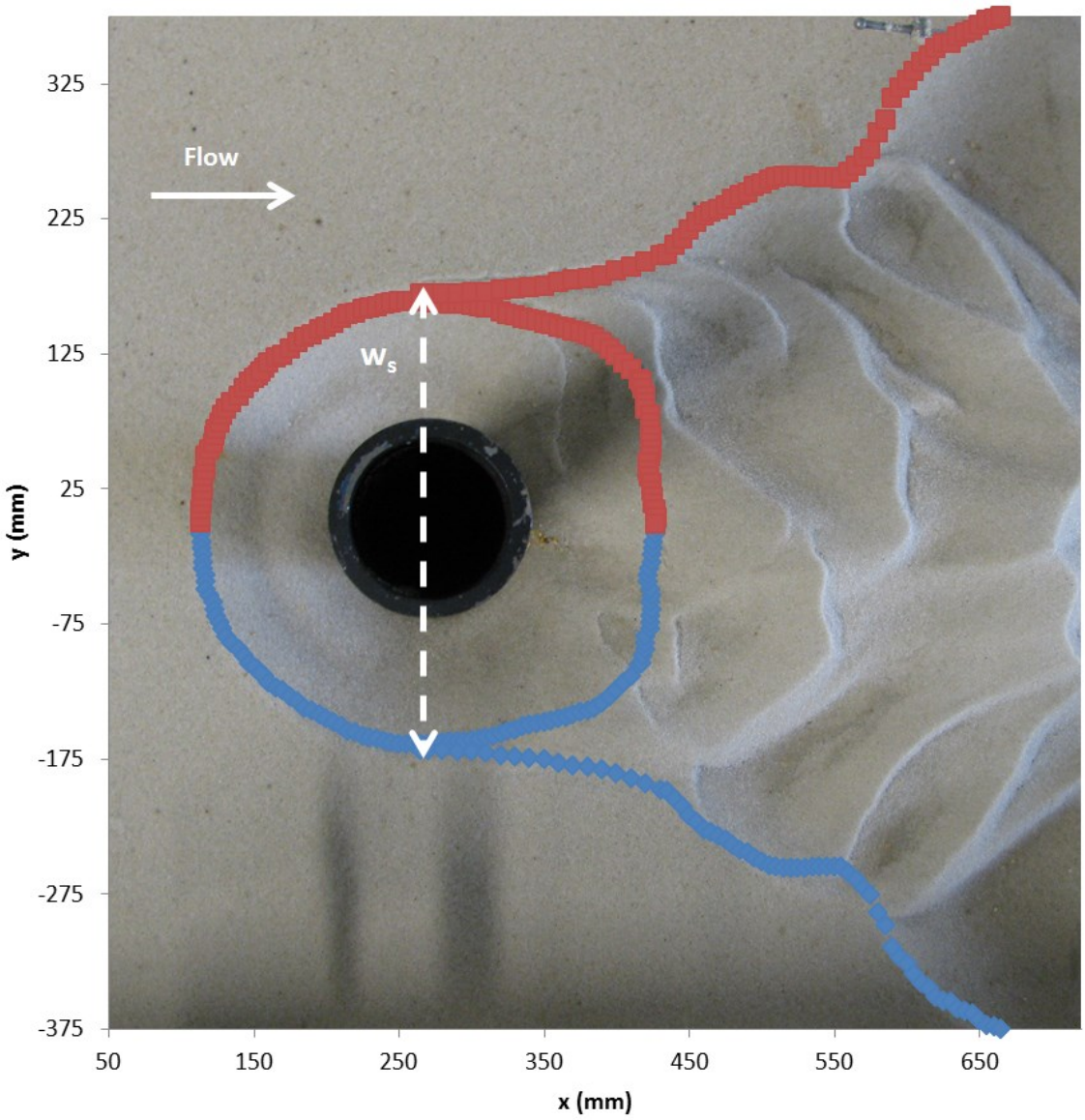

Figure 3.5. Point measurements of the contour profile of a scour hole

CHAPTER 4

RESULTS AND DISCUSSION

4.1. Overview

This discussion will open with results on each phase of experimentation (as outlined in **Section 3**); the first phase (consisting of series A and B) is focused on isolation of D/d_{50} influences, while the second phase (series E and F) was performed with the intention of isolating the influence of h/D on scour depth. This will be followed by a description of the development of and presentation of a new scour prediction method based on these and prior results acquired during experimentation at the University of Windsor by D'Alessandro (2013) and Tejada (2014).

4.2. Phase I: Relative Coarseness, D/d_{50}

The results of the first phase of testing are shown in **Table 4.1**, including equilibrium scour depth (d_{se}), relative scour depth (d_{se}/D), width of scour hole (w_s), and relative width of scour hole (w_s/D), which were described in **Section 3.4**. As previously described in **Section 3.2**, series "A" and series "B" each consisted of six tests.

Tests A1 through A6 were conducted using bed material with a mean diameter of 0.51 mm; for each test, pier diameter D was changed. Flume width b and water height h were scaled based on this changing D, in order to maintain constant flow shallowness (h/D) and blockage (D/b). Thus, the only varying primary non-dimensional parameter became relative coarseness (D/d_{50}). The majority of controlled parameters (h, D, b, and U/U_c) in tests B1 through B6 were identical to tests A1 through A6; only d_{50} (which was 0.77 mm in series B) was changed.

Table 4.1: Phase 1 Experimental Results

Test ID	D (m)	d_{50} (mm)	h (m)	b (m)	U (m/s)	d_{se} (cm)	d_{se}/D	w_s (cm)	w_s/D	D/d_{50}
A1	0.121	0.51	0.193	1.22	0.224	9.06	0.751	49.4	4.09	237
A2	0.101	0.51	0.161	1.02	0.224	7.12	0.706	41.4	4.11	198
A3	0.089	0.51	0.142	0.90	0.224	6.73	0.757	36.7	4.13	174
A4	0.079	0.51	0.127	0.80	0.224	6.43	0.810	32.7	4.12	156
A5	0.070	0.51	0.112	0.71	0.224	6.23	0.892	32.2	4.61	137
A6	0.060	0.51	0.096	0.61	0.224	5.87	0.974	29.4	4.88	118
B1	0.121	0.77	0.193	1.22	0.259	7.51	0.622	43.4	3.60	157
B2	0.101	0.77	0.161	1.02	0.259	8.18	0.812	43.5	4.32	131
B3	0.089	0.77	0.142	0.90	0.259	7.26	0.817	37.9	4.26	115
B4	0.079	0.77	0.127	0.80	0.259	7.00	0.882	35.4	4.46	103
B5	0.070	0.77	0.112	0.71	0.259	6.29	0.901	32.9	4.71	91
B6	0.060	0.77	0.096	0.61	0.259	5.70	0.946	26.6	4.41	78

The dimensionless centreline and contour scour profiles for tests A1 through A6 are shown in **Figures 4.1** and **4.3**, respectively, and profiles for tests B1 through B6 are shown in **Figure 4.2** and **4.4**. The origin for each profile is located at the geometric centre of the pier. The x-axis is in the direction of flow, the y-axis is transverse to the flow, and the z-axis is normal to the x and y axes.

Figures 4.1 and **4.2** demonstrate that tests with varying D/d_{50} and constant h/D, D/b, and U/U_c yield similar scour profiles. All tests with d_{50} = 0.77 mm resulted in scour profiles with primary sediment deposits downstream of the pier, and the lengths of these deposits were all less than six pier diameters (6D). Here, deposit length refers to the distance between the first two points at which the centreline profile crosses or reaches the x-axis. Primary sediment deposits for all tests with d_{50} = 0.51 mm were longer than 6D; in addition, these deposits all consisted of bed formations in the form of ripples, which is typical for sediment finer than 0.70 mm.

While the influences of D/d_{50} on scour geometry upstream of the pier were found to be small physically and quantitatively (**Table 4.1**, **Figures 4.1** and **4.2**), the downstream section of each centreline profile showed greater changes for tests with varying values of D/d_{50}. This is illustrated in **Figure 4.2**, where the relative scour depth at the downstream face of the pier generally increases with decreasing D/d_{50}.

As previously described (**Section 2**), flow velocity increases around the pier from a stagnation point on its upstream face, where U = 0 and pressure is at a maximum. This velocity reaches a maximum value at the point of separation, where the streamline leading from the stagnation point around the pier in the downstream direction detaches from the pier. This velocity, known as separation velocity or U_s, is highly influential on scour depth, as scouring action is initiated at the location on the pier face where this separation occurs. Separation velocity is a function of base pressure on the downstream face of the pier, and can therefore be determined when the base pressure coefficient is known (Roshko, 1961; Norberg, 1987). It is important to note that U_s has been identified as the proper velocity scale and blockage effects can be reduced or eliminated by the use of U_s in the case of flow past bluff bodies (Ramamurthy, 1973). As shown in **Section 4.5**, the magnitude of U_s changes with changing D. It follows from the above-observation that if changes in D/d_{50} are pronounced in the downstream section of the scour hole, then the effects of changes in U_s are also magnified downstream of the point of separation.

As with the centreline profiles for the A and B tests, **Figures 4.3** and **4.4** show that, in tests with varying D/d_{50} and all other primary non-dimensional parameters held constant, contour profiles are very similar. However, this does not apply to tests with changing values of d_{50}.

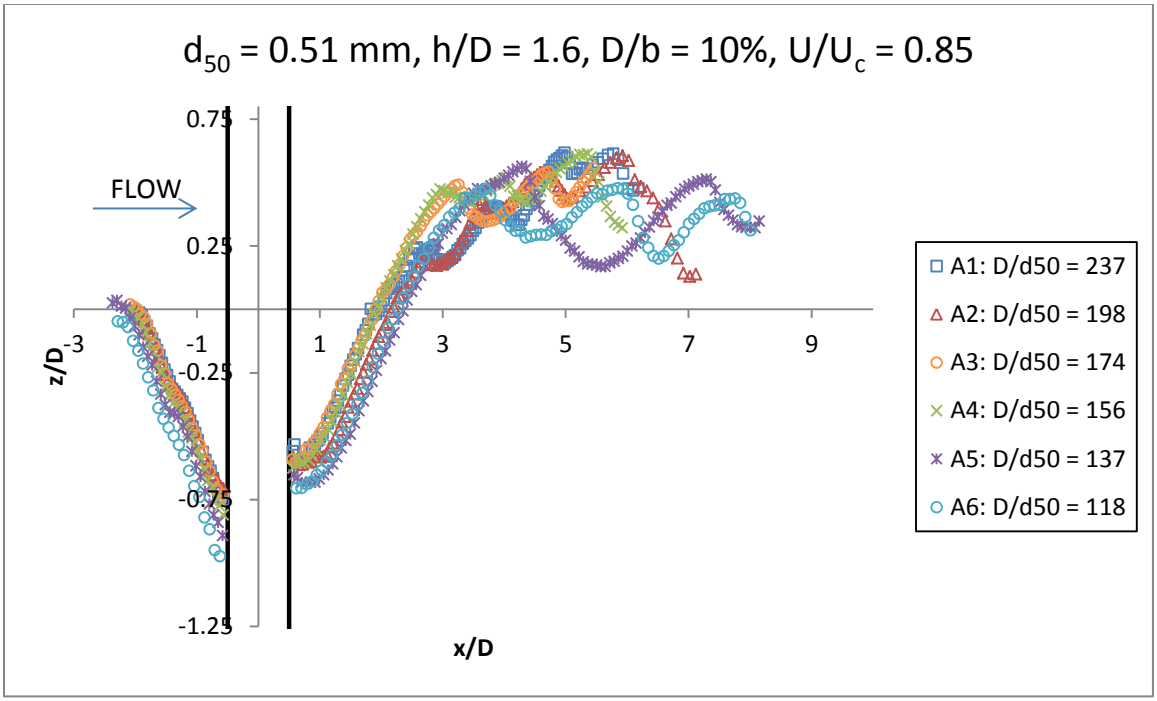

Figure 4.1. Centreline profiles for phase I, series A tests (constant h/D, D/b, U/U_c)

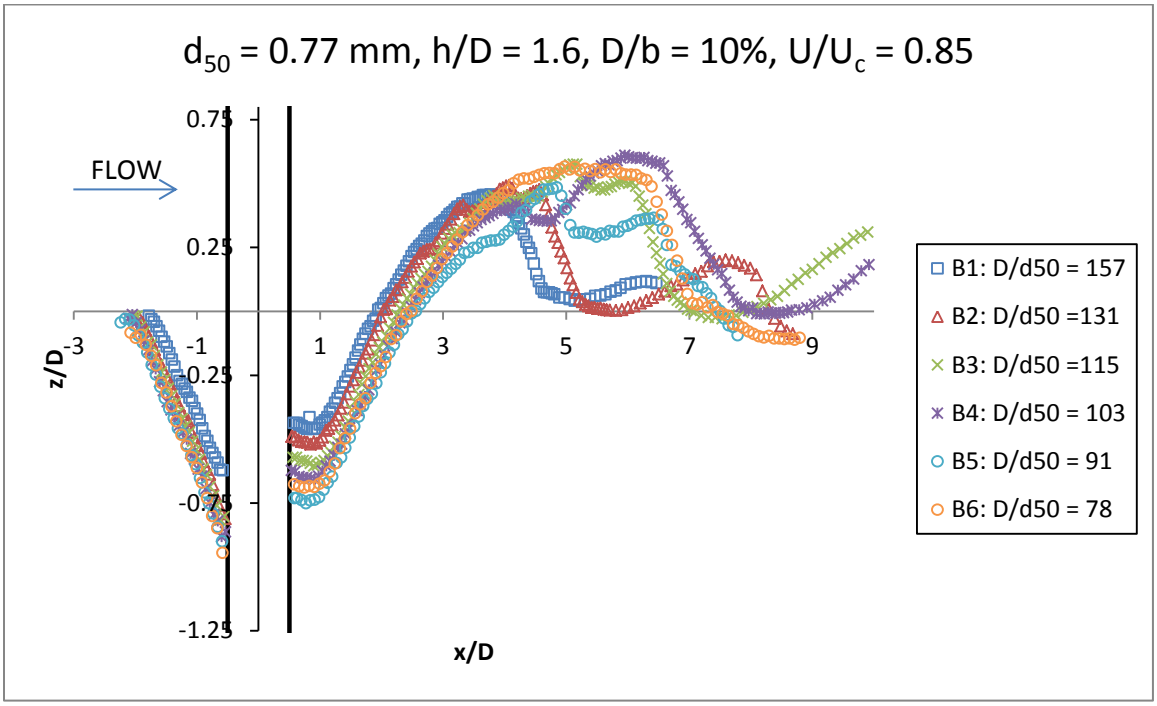

Figure 4.2. Centreline profiles for phase I, series B (constant h/D, D/b, U/U_c)

In **Figure 4.3**, scour profiles for tests A1 through A6 (d_{50} = 0.51 mm) reached the sidewalls of the channel, indicating that despite a constant blockage ratio of 10 percent,

secondary currents due to wall interference affected scouring action. However, for tests B1 through B6 (d_{50} = 0.77 mm), none of the scour profiles extended as far as the sidewalls. Therefore, scour in beds with finer sediment are more greatly affected by wall interference. For tests A1 through A6, scour generally reached the sidewalls at a lesser distance downstream of the pier for greater values of D/d_{50}, indicating that wall interference also affects sediment-structure interactions. Therefore, if all other non-dimensional parameters are constant between series A and series B, it follows that blockage influences must increase with some additional sediment-related non-dimensional parameter.

Figures 4.5 and **4.6** show that the maximum scour depth and scour width both decrease consistently with increasing D/d_{50} values, confirming the influence of D/d_{50} on equilibrium scour depth described by Lee and Sturm's (2009) trendline. However, for greater values of D/d_{50} (>175), d_{se}/D is relatively constant, suggesting that the effects of relative coarseness are dampened at this range. This relationship between d_{se}/D and D/d_{50} is very clearly shown by the results in series A and series B when each series is viewed separately.

Between series A and series B, there are pairs of tests with very similar values of D/d_{50} (represented by dotted ellipses in **Figures 4.5** and **4.6**); for example, B3 with D/d_{50} = 115 and A6 with D/d_{50} = 118, B2 with D/d_{50} = 131 and A5 with D/d_{50} = 137, or B1 with D/d_{50} = 157 and A4 with D/d_{50} = 156. Among these tests, all other primary non-dimensional parameters (h/D, U/U_c, etc.) are held constant. Therefore, if D/d_{50} were indeed the only remaining non-dimensional parameter of influence, then it would follow

that pairs of tests with such close values of D/d_{50} should have values of d_{se}/D that are also very close in magnitude and scour profiles that are nearly identical.

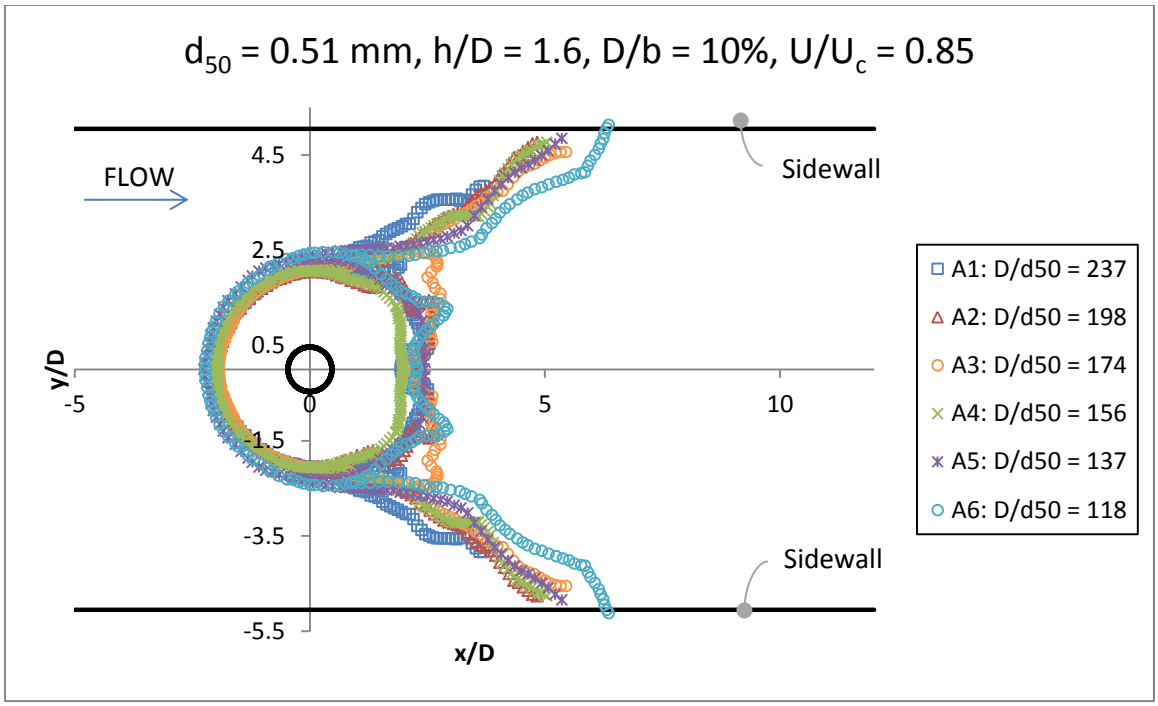

Figure 4.3. Contour profiles for phase I, series A (constant h/D, D/b, U/U_c)

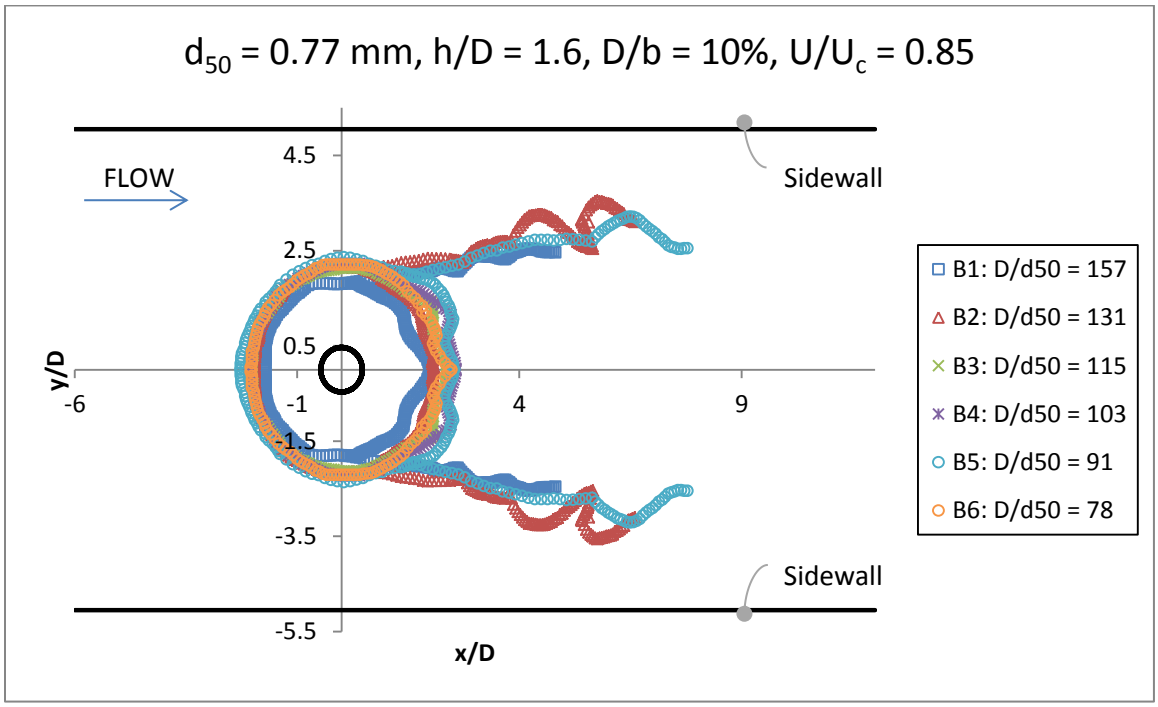

Figure 4.4. Contour profiles for phase 1, series B (constant h/D, D/b, U/U_c)

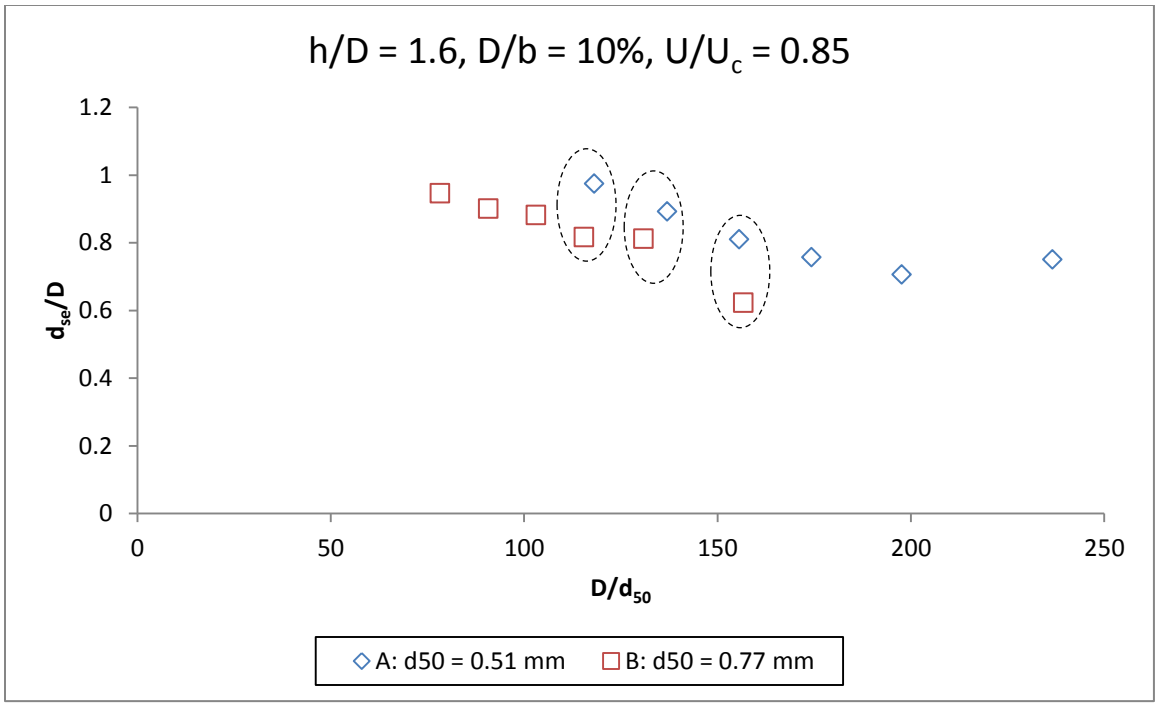

Figure 4.5. Variation of d_{se}/D with relative coarseness for phase I (constant h/D, D/b, U/U_c)

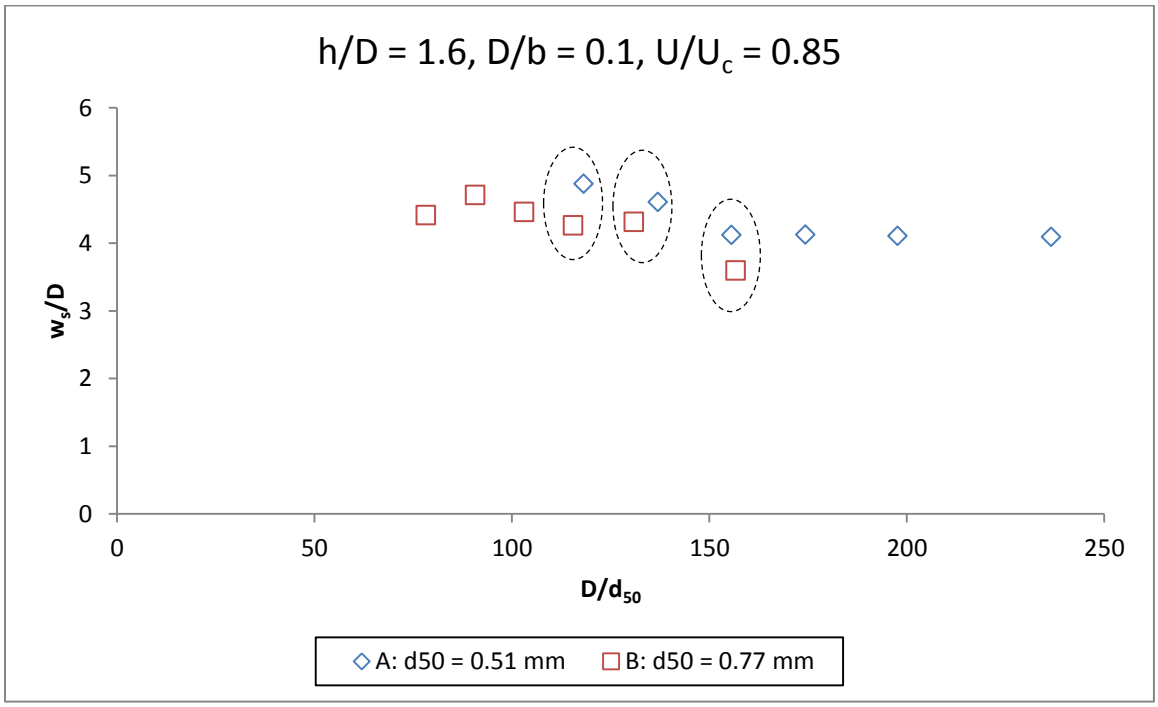

Figure 4.6. Variation of w_s/D with relative coarseness for phase I (constant h/D, D/b, U/U_c)

As demonstrated by **Figures 4.7** and **4.8**, this assumption does not prove true. Comparison of profiles from each pair of tests indicates that changes exist in d_{se}/D and

w_s/D between tests of different sediment size, despite near-constant D/d_{50}. This indicates, again, that there is another sediment-related non-dimensional parameter which influences the scouring process; through further analysis of results (to be discussed below in **Section 4.5**), this was determined to be the densimetric Froude number, F_d. Defined in **Equation 4.1**, the densimetric Froude number is representative of the ratio between the inertial force on each bed particle and its submerged specific weight (Hodi, 2009).

$$F_d = \frac{U}{\sqrt{g(SG-1)d_{50}}} \qquad \textbf{[4.1]}$$

As previously discussed, the contour profiles of all series A tests in these comparative figures show that scouring action reached the sidewalls which, again, did not occur for any of the corresponding series B tests; this confirms that blockage effects are variable with changing d_{50} and therefore F_d.

For tests in series A and series E (d_{50} = 0.51 mm), F_d was calculated to be 2.40. For tests in series B and F (d_{50} = 0.77 mm), F_d was calculated to be 2.30. Therefore, effects of wall interference from blockage increase with increasing F_d. Furthermore, when all other non-dimensional parameters are held constant, d_{se}/D decreases with decreasing F_d.

In conclusion, it has been determined that d_{se}/D decreases with increasing D/d_{50} until a limiting value of D/d_{50} = 175, after which d_{se}/D reaches a constant value of approximately 0.75, which is in agreement with Lee and Sturm's (2009) trendline. In addition, the densimetric Froude number (representative of flow-sediment interactions) and separation velocity (representative of wall interference due to blockage) have been shown to affect d_{se}/D.

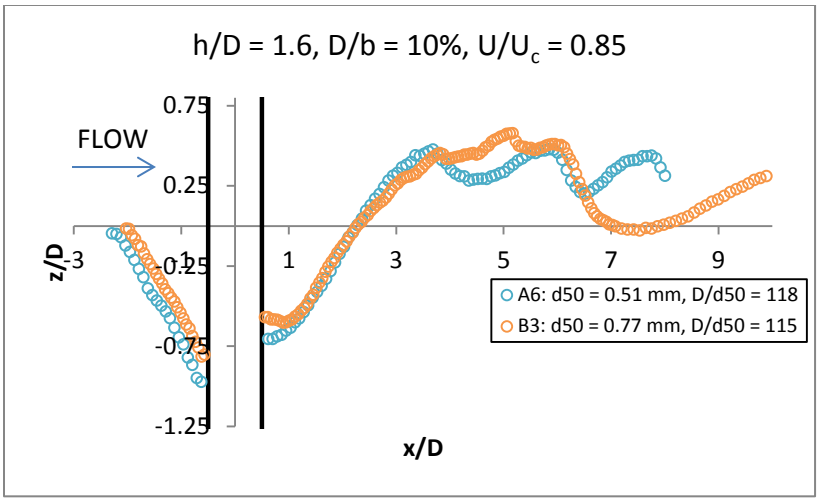

[a]

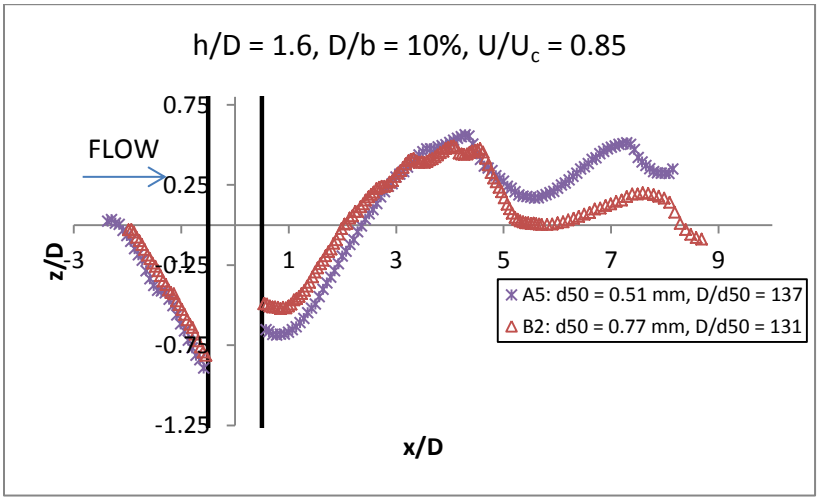

[b]

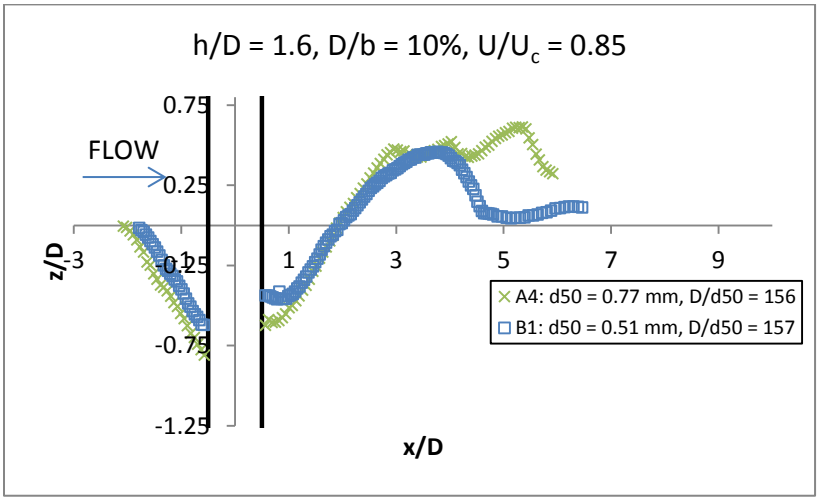

[c]

Figure 4.7. Comparison of centreline profiles for phase I: [a]A6/B3, [b]A5/B2, [c]A4/B1

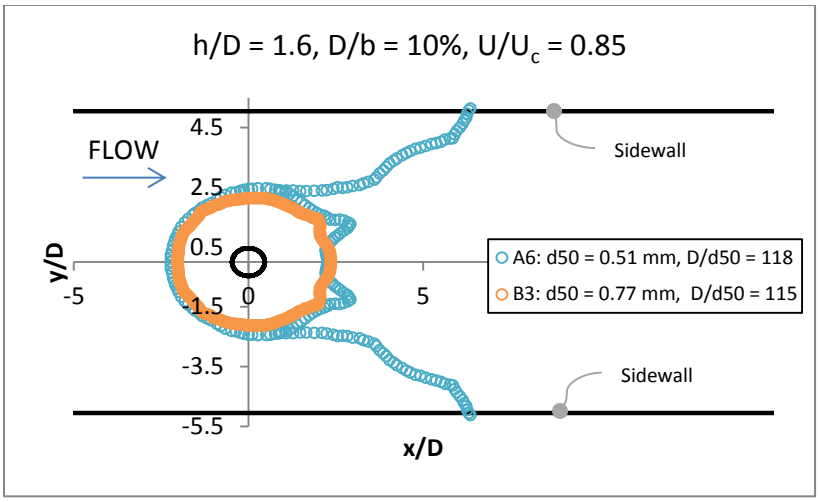

[a]

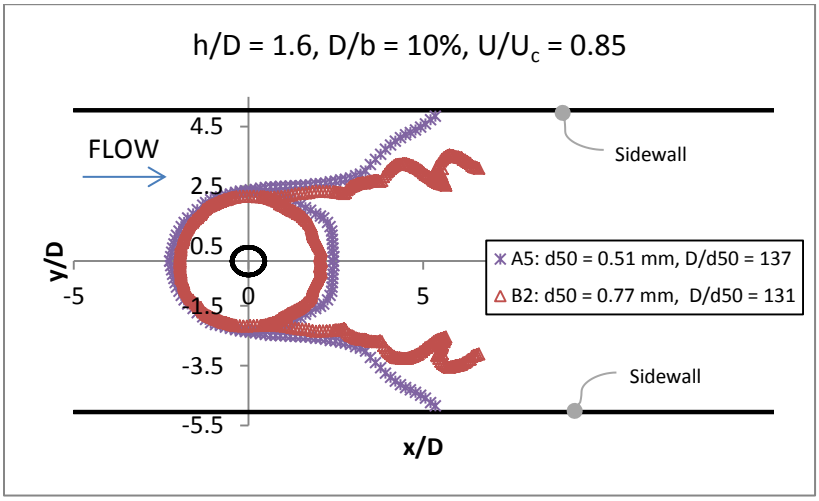

[b]

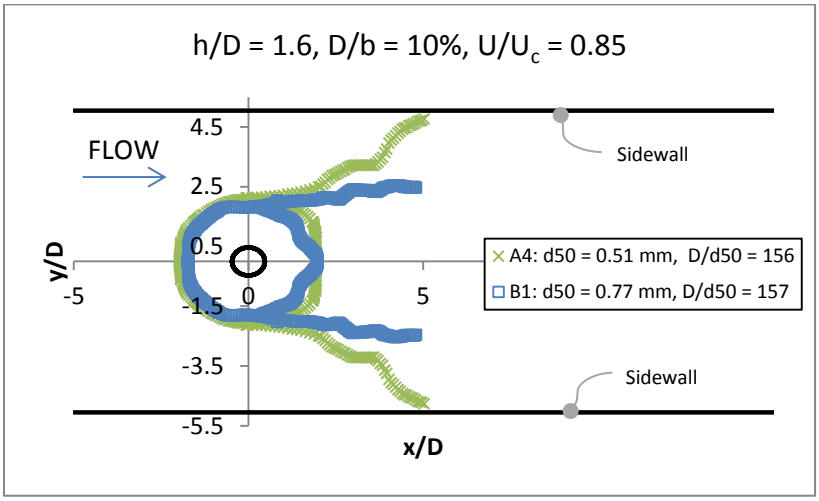

[c]

Figure 4.8. Comparison of contour profiles for phase I: [a]A6/B3, [b]A5/B2, [c]A4/B1

4.3. Phase II: Flow Shallowness, h/D

Table 4.2 shows experimental results for the second phase of testing, which consists of two series, "E" and F". The majority of test conditions in series E were the same as those of test A6, with increasing values of water height, h. Because test A6 had the lowest water depth of the tests in series A, this allowed for the largest achievable range of h/D values should h be increased to the maximum that the laboratory facilities would allow while still maintaining $U/U_c = 0.85$. Therefore, by holding d_{50}, D/d_{50}, D/b, and U/U_c constant, the influences of h/D on scour were isolated for each series. Similarly, test conditions in series F were identical to those of test B6, with the exception of flow shallowness h/D.

Table 4.2: Phase II Experimental Results

Test ID	D (m)	d_{50} (mm)	h (m)	b (m)	U (m/s)	d_s (cm)	d_{se}/D	w_s (cm)	w_s/D	h/D
E1	0.060	0.51	0.240	0.61	0.224	8.75	1.452	42.3	7.02	4.0
E2	0.060	0.51	0.192	0.61	0.224	9.56	1.587	48.0	7.97	3.2
E3	0.060	0.51	0.144	0.61	0.224	10.23	1.698	48.4	8.03	2.4
E4	0.060	0.51	0.120	0.61	0.224	10.08	1.673	44.0	7.30	2.0
E5	0.060	0.51	0.112	0.61	0.224	8.40	1.394	39.0	6.47	1.9
E6	0.060	0.51	0.085	0.61	0.224	7.21	1.197	34.2	5.68	1.4
F1	0.060	0.77	0.241	0.61	0.259	7.57	1.256	32.4	5.38	4.0
F2	0.060	0.77	0.193	0.61	0.259	9.78	1.623	44.6	7.40	3.2
F3	0.060	0.77	0.145	0.61	0.259	9.33	1.549	43.0	7.14	2.4
F4	0.060	0.77	0.120	0.61	0.259	9.55	1.585	40.8	6.77	2.0
F5	0.060	0.77	0.096	0.61	0.259	5.70	0.946	26.6	4.41	1.6

Figures 4.9 through **4.12** show the centreline and contour profiles of scour for all tests in series E and F. As with the tests in phase I, **Figures 4.9** and **4.10** show that scour profiles for tests with increasing h/D are similar in form. For tests with $d_{50} = 0.51$ mm, the majority of primary sediment deposits are of shorter relative length than for tests with $d_{50} = 0.77$ mm. Bed ripples are also present on the primary deposits for the series E tests.

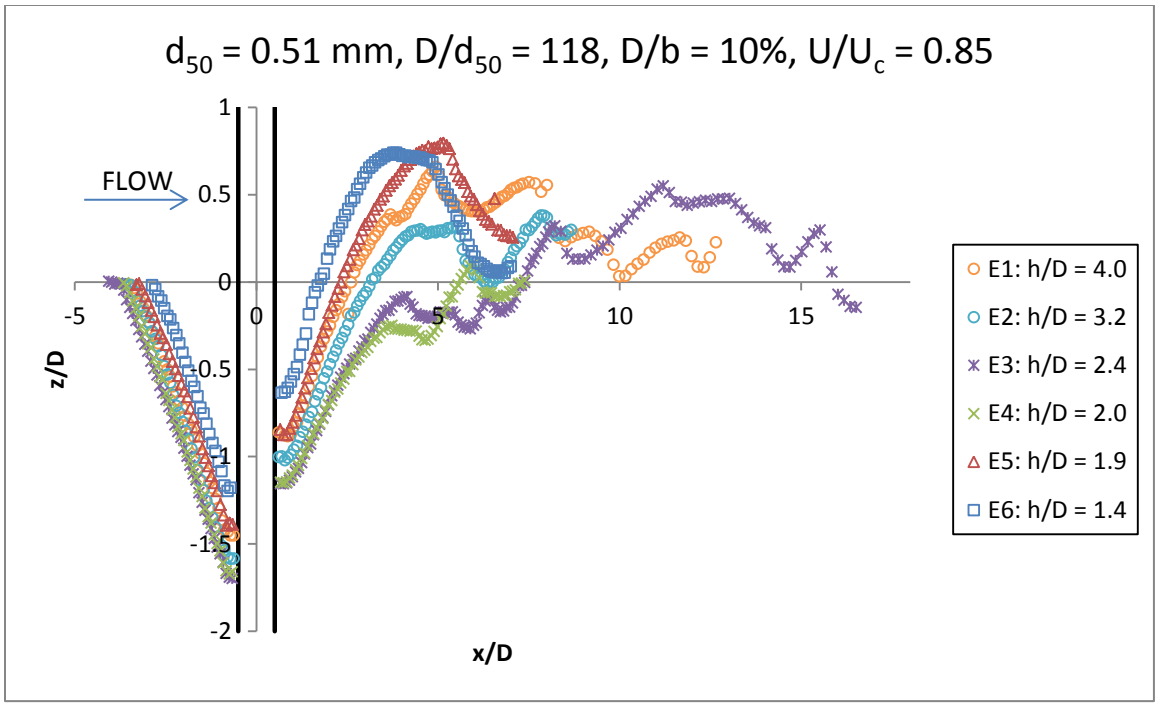

Figure 4.9. Centreline profiles for phase II, series E (constant h/D, D/b, U/U_c)

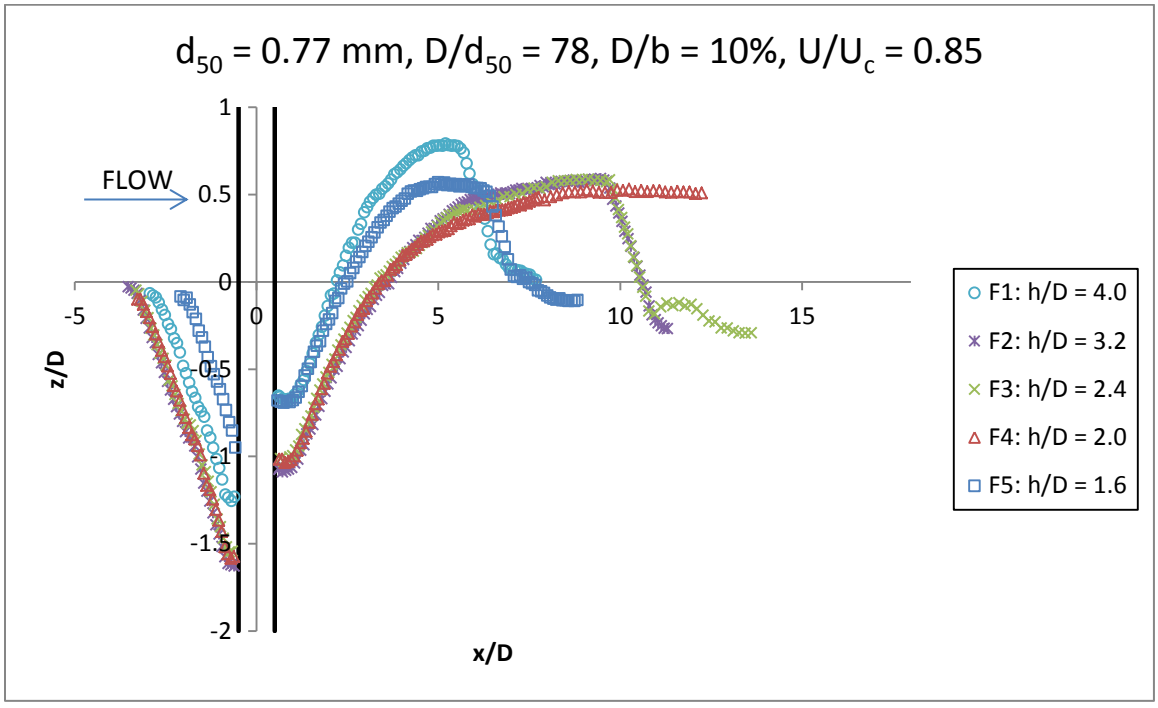

Figure 4.10. Centreline profiles for phase II, series F (constant h/D, D/b, U/U_c)

The effects of wall interference are once again demonstrated by the contour profile superposition in **Figures 4.11** and **4.12**. In tests E1 through E6 (d_{50} = 0.51 mm,

D/d_{50} = 118), scour reaches the sidewalls at a shorter distance downstream than in tests F1 through F5 (d_{50} = 0.51 mm, D/d_{50} = 78), indicating again that the effects of wall interference are increased in smaller sediment. Therefore, blockage is shown to have a greater influence on sediment-structure interactions with increasing D/d_{50} values, as was demonstrated by phase 1 tests as well.

In series E and series F, scour in tests with increasing h/D reached the sidewalls at a shorter distance downstream until h/D = 4.0, at which point the relative size and depth of the scour hole decreased and scour reached the sidewalls at a further distance downstream of the pier. Similarly, scour for the two tests of lowest d_{se}/D in series F (F5 and F1; shown in **Table 4.2** and **Figure 4.12**) failed to reach the sidewalls altogether. Therefore, effects of wall interference increase with increasing h/D, until a limiting value of h/D = 3.2.

Figures 4.13 and **4.14** show the graphical relationship between flow shallowness and relative scour depth as well as relative scour width. Both figures show that d_{se}/D and w_s/D generally increase with increasing h/D until a limiting value of 3.2, after which d_{se}/D appears to decrease. This is confirmed by the scour profiles shown in **Figure 4.9** through **4.12**; the centreline and contour profiles for tests 2,3, and 4 (h/D = 2, 2.4, and 3.2, respectively) in both series E and series F are similar, and scour depth and width in this range of h/D values is nearly constant. However, h/D still appears to have an influence beyond a value of h/D = 3.2; for tests with an h/D of 4.0 (E1 and F1), scour appears to decrease. This disagrees with Melville and Coleman's (2000) trendline, which indicates that h/D no longer affects scour beyond a limiting value of h/D = 1.4 (above

which piers are classified as narrow). Therefore, this classification alone does not exempt scour from the influences of flow shallowness.

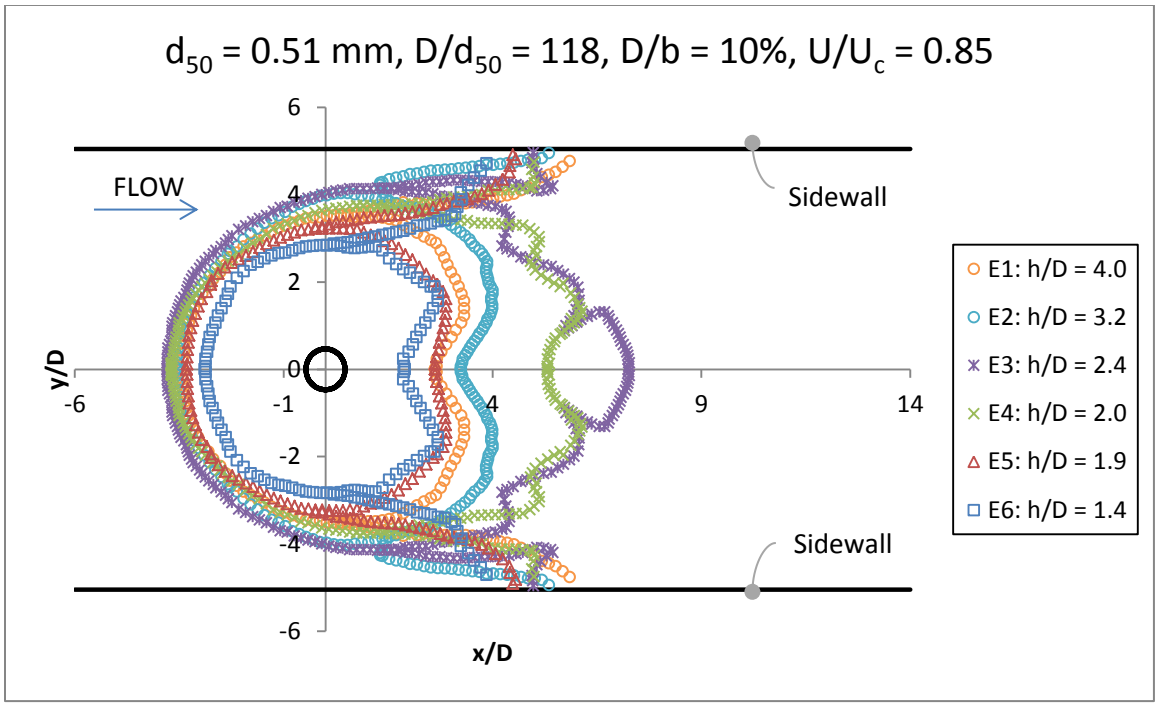

Figure 4.11. Contour profiles for phase II, series E (constant h/D, D/b, U/U_c)

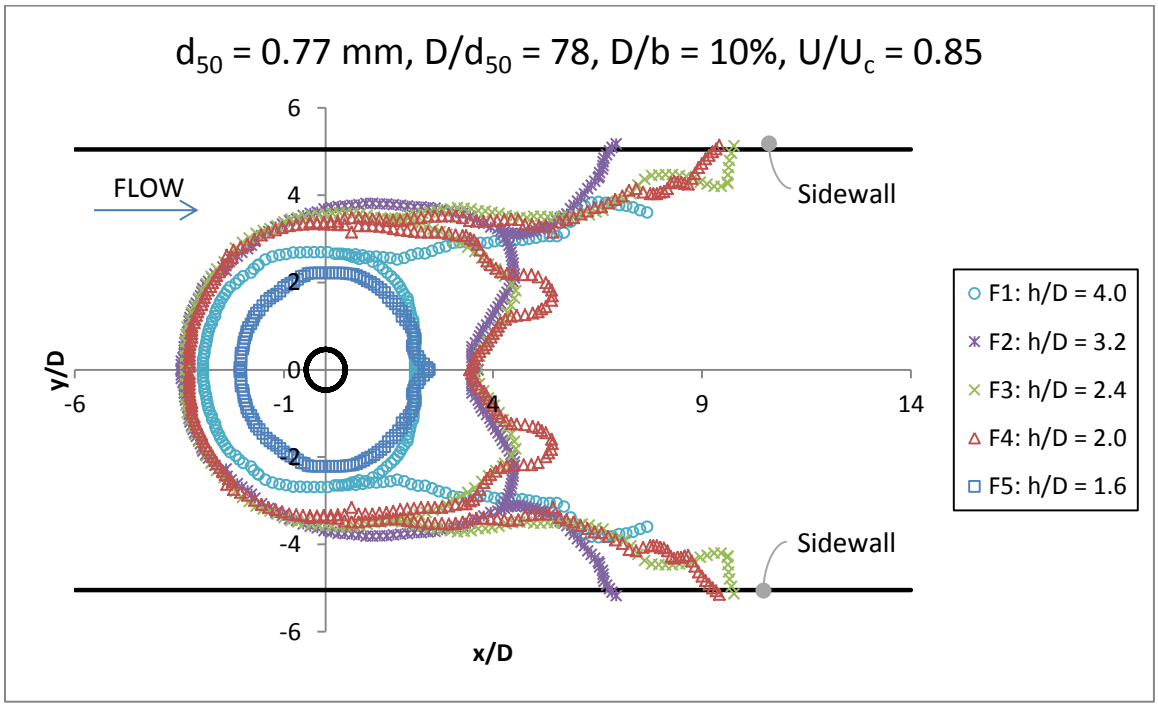

Figure 4.12. Contour profiles for phase II, series F (constant h/D, D/b, U/U_c)

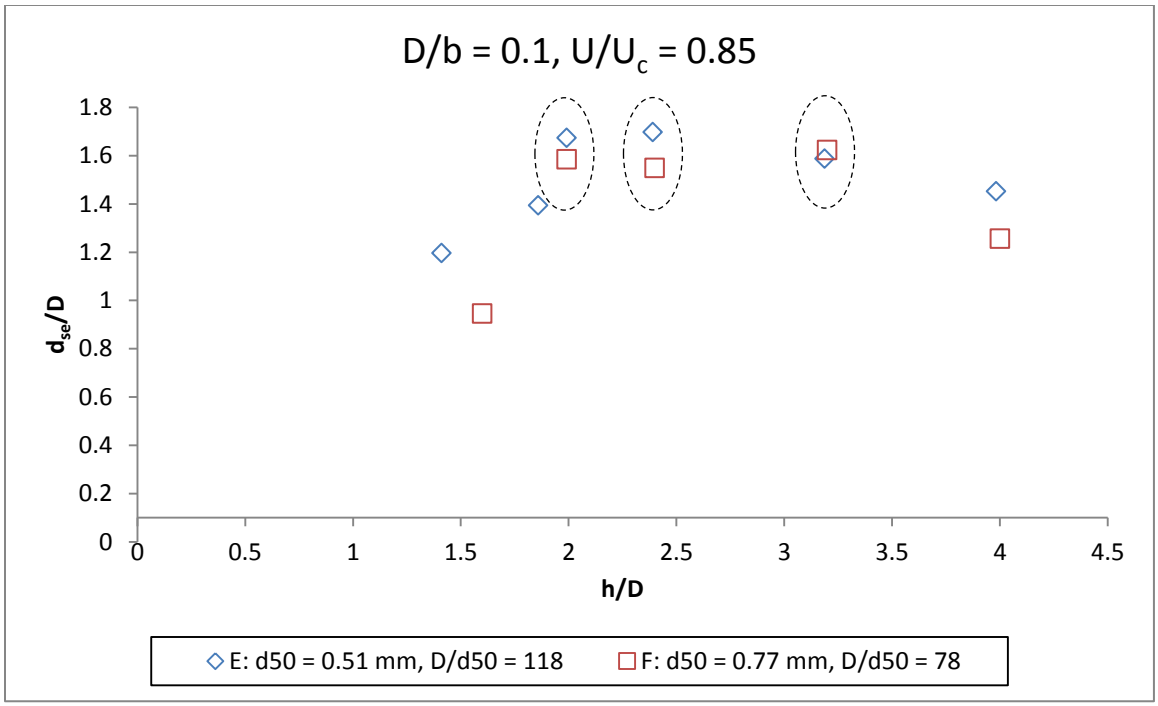

Figure 4.13. Variation of d_{se}/D with flow shallowness for phase II (constant h/D, D/b, U/U_c)

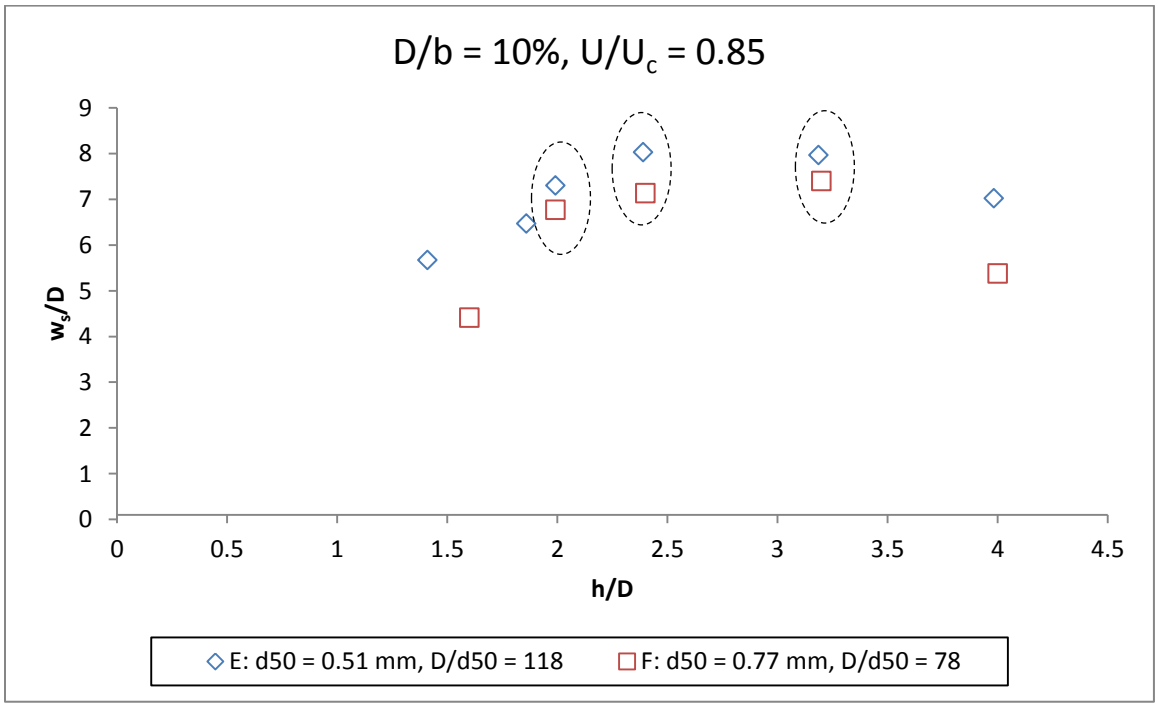

Figure 4.14. Variation of w_s/D with flow shallowness for phase II (constant h/D, D/b, U/U_c)

Melville and Coleman (2000) introduced a system of pier designation based on values of h/D, such that narrow piers were defined as those with h/D values greater than

1.4; scour around piers of a narrow classification is highly dependent on pier diameter D. In the intermediate range of piers ($0.2 \leq h/D \leq 1.4$), the square root of hD has the greatest influence on d_{se}. Finally, in the wide range of piers, for which h/D is less than 0.2, water height has the greatest influence on scour. According to these definitions, the value of d_{se}/D for h/D values greater than 1.4 should indeed be constant, regardless of water height (Ettema et al., 2011). However, series E and F results in phase II of testing indicate that d_{se}/D does fluctuate with increasing values of h/D beyond 1.4, refuting the convention that high values of h/D do not influence scour.

When comparing series E and series F, there are dissimilarities in scour even in tests with constant h/D. **Figures 4.15** and **4.16** show scour profiles for three pairs of tests (E2 and F2, E3 and F3, and E4 and F4), in order to show comparison in tests with varying D/d_{50} at higher h/D values. These figures indicate that the effects of D/d_{50} on d_{se}/D are reversed at higher values of h/D. In series A and B, with h/D = 1.6 for all tests, d_{se}/D consistently decreased with increasing D/d_{50} until a limiting value of $D/d_{50} = 175$, after which the relationship between the two parameters reached constancy. However, these comparative figures indicate that at higher values of h/D, relative scour is greater in depth and profile for tests with $D/d_{50} = 118$ when compared with the same for tests with $D/d_{50} = 78$.

As with phase I tests, the differences in scour geometry downstream of the pier between tests in different sands are highlighted above. In **Figures 4.15** and **4.16**, the centreline and contour profile comparisons for each pair of tests shows that scour upstream of the pier is very similar (and in the case of E2 and E4, nearly identical). **Table**

4.2, **Figures 4.13** and **4.14** also show that maximum scour depth and width for these tests are similar, with d_{se}/D and w_s/D for series F tests being slightly lesser.

In **Figure 4.15**, the primary deposits for series E tests with d_{50} = 0.51 mm (F_d = 2.40) are shown to be significantly different from those for series F tests with d_{50} = 0.77 mm (F_d = 2.30). In **Figure 4.15[b]** and **[c]**, the length of the scour holes in E3 and E4 are greater than the length of the scour holes in F3 and F4, and bed ripples begin to form within the hole itself. In **Figure 4.15[a]**, where the length of the scour holes for both tests E2 and F2 are very similar, the form and height of the primary deposit itself is still very different.

In **Figure 4.16**, the effects of sidewall interference on scour can be seen. In each figure, point B2 is the point at which the figure's series F test reaches the sidewall; point B1 is the point at which the figure's series E test reaches the sidewall. In all cases, B2 is located at a greater distance downstream of the pier than B1, indicating again that the effects of wall interference on scouring action are greater in smaller sediment (or greater F_d, in the case of phase II tests), despite constant h/D, D/b and U/U_c.

In conclusion, d_{se}/D increases with increasing h/D for h/D values above 1.4, until the range of h/D between 2.0 and 3.2. Over this range, d_{se}/D is constant; however, d_{se}/D decreases again for values of h/D greater than 3.2. Therefore, Melville and Coleman's (2000) trendline (for which d_{se}/D is constant for h/D beyond 1.4) is not valid when the influences of h/D are isolated. The influence of wall interference on scour is also more pronounced for tests with greater values of densimetric Froude number (F_d), even with h/D, D/b and U/U_c held constant.

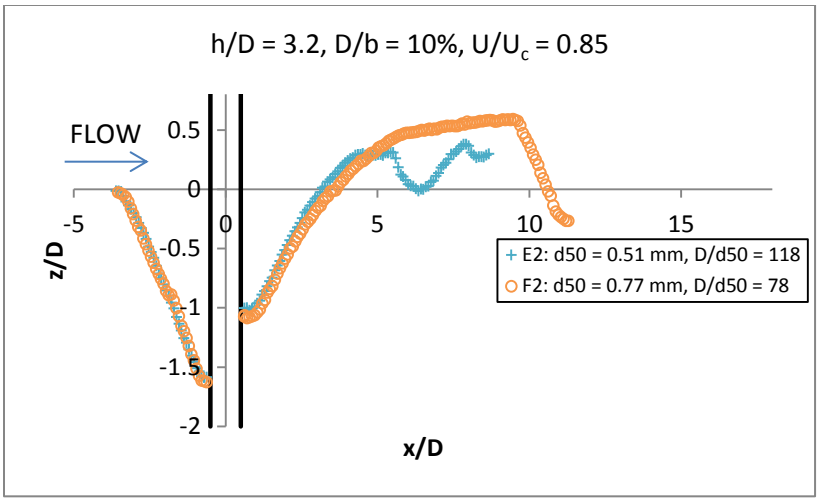

[a]

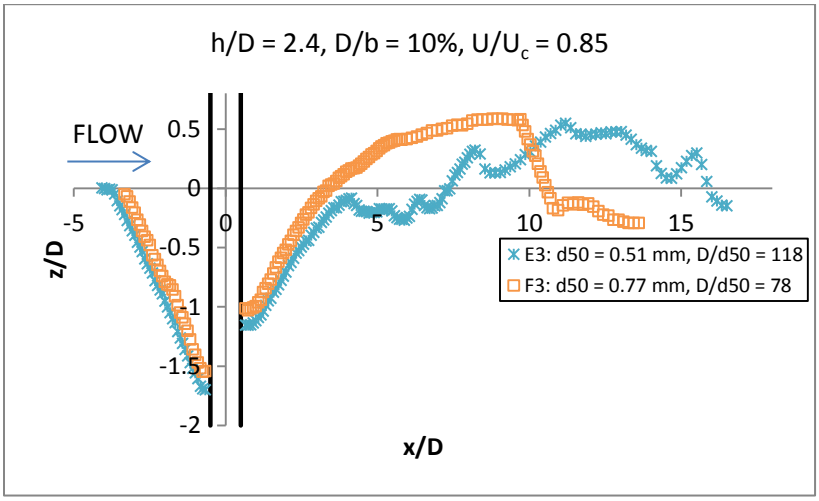

[b]

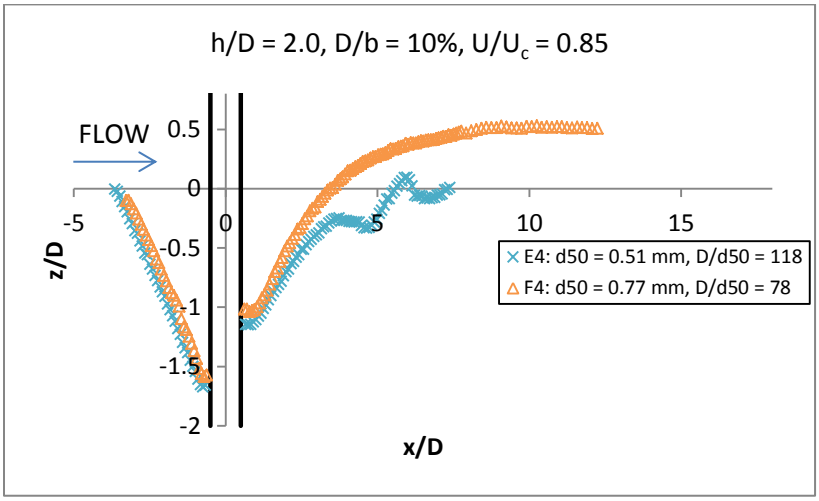

[c]

Figure 4.15. Comparison of centreline profiles for phase II: [a]E2/F2, [b]E3/F3, [c]E4/F4

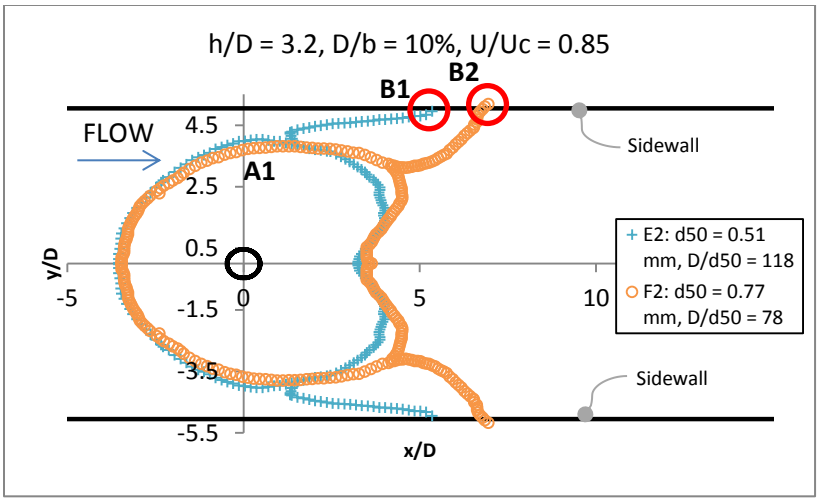

[a]

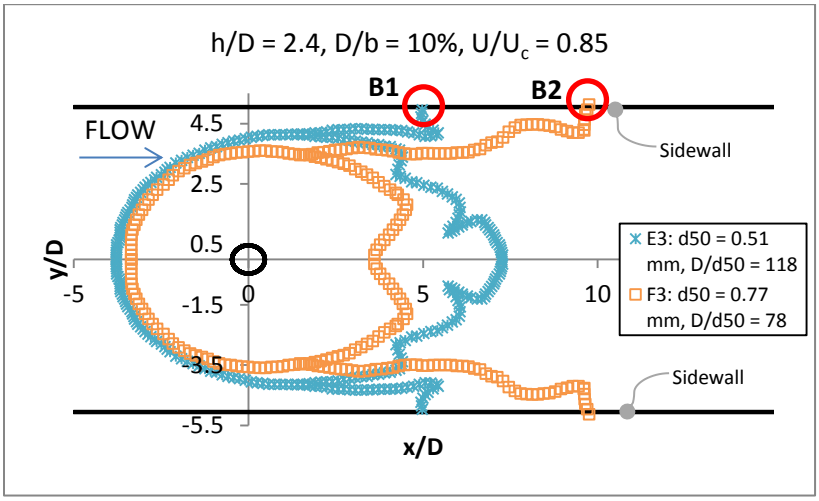

[b]

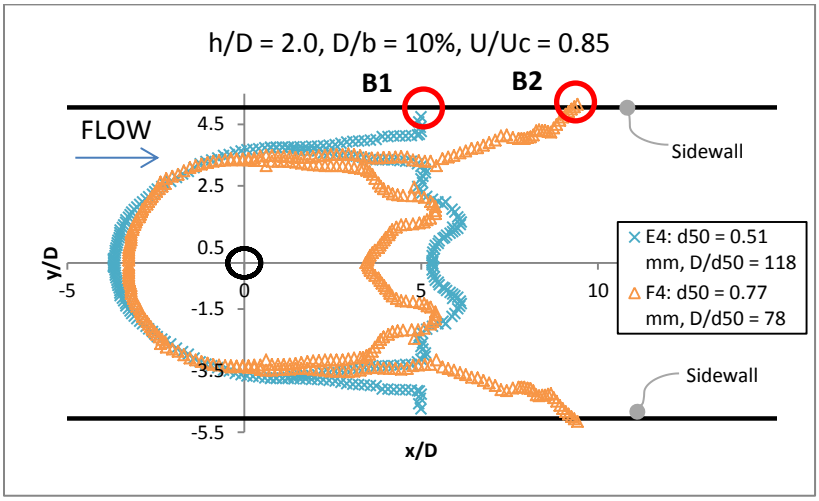

[c]

Figure 4.16. Comparison of contour profiles for phase II: [a]E2/F2, [b]E3/F3, [c]E4/F4

4.4. University of Windsor Results: Blockage Ratio, D/b

Figures 4.18 through **4.23** show scour profiles for series E and F tests compared with results from previous University of Windsor experimentation with similar test parameters. **Figures 4.17** through **4.19** compare test E4 (F_d = 2.40) with test E16 (F_d = 2.62) from D'Alessandro's (2013) investigation on blockage effects. The test conditions for E4 and D'Alessandro's test E16 are identical, with the exception of blockage ratio, which is 5% for E16, and densimetric Froude number. Comparison of these two tests shows that, for tests with d_{50} = 0.51 mm, d_{se}/D increases with increasing blockage.

Figure 4.17 demonstrates the effects of sidewall interference on scour; in D'Alessandro's (2013) test (D/b = 5%), scour does not reach the sidewalls until a significantly longer length downstream than for E4 (D/b = 10%). With all other non-dimensional parameters held constant (except the densimetric Froude number), sidewall proximity is the only remaining variable that accounts for changes in scour between these two tests. As demonstrated by **Figure 4.19**, scour in the test with a higher blockage ratio is deeper, wider, and longer than scour with a smaller D/b.

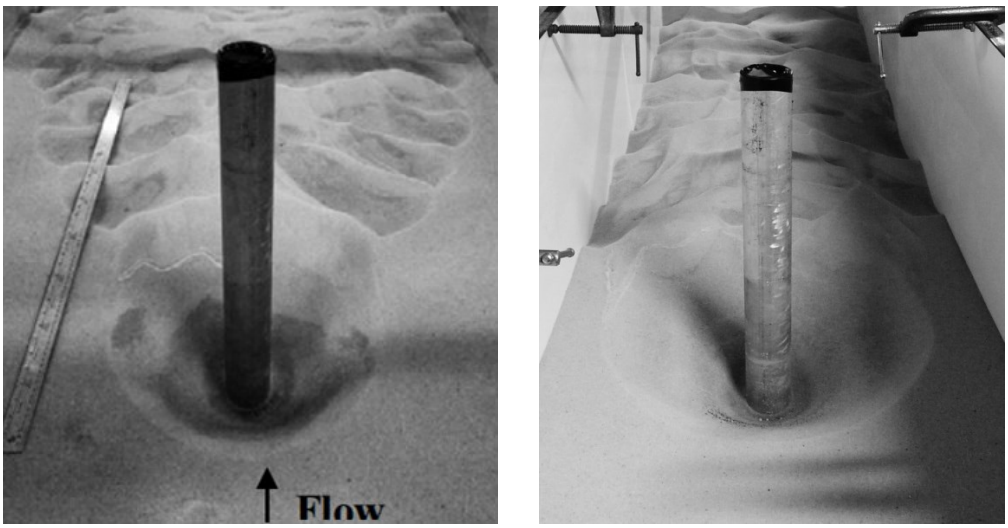

Figure 4.17. Upstream view of D'Alessandro's (2013) E16 test (left) and E4 (right)

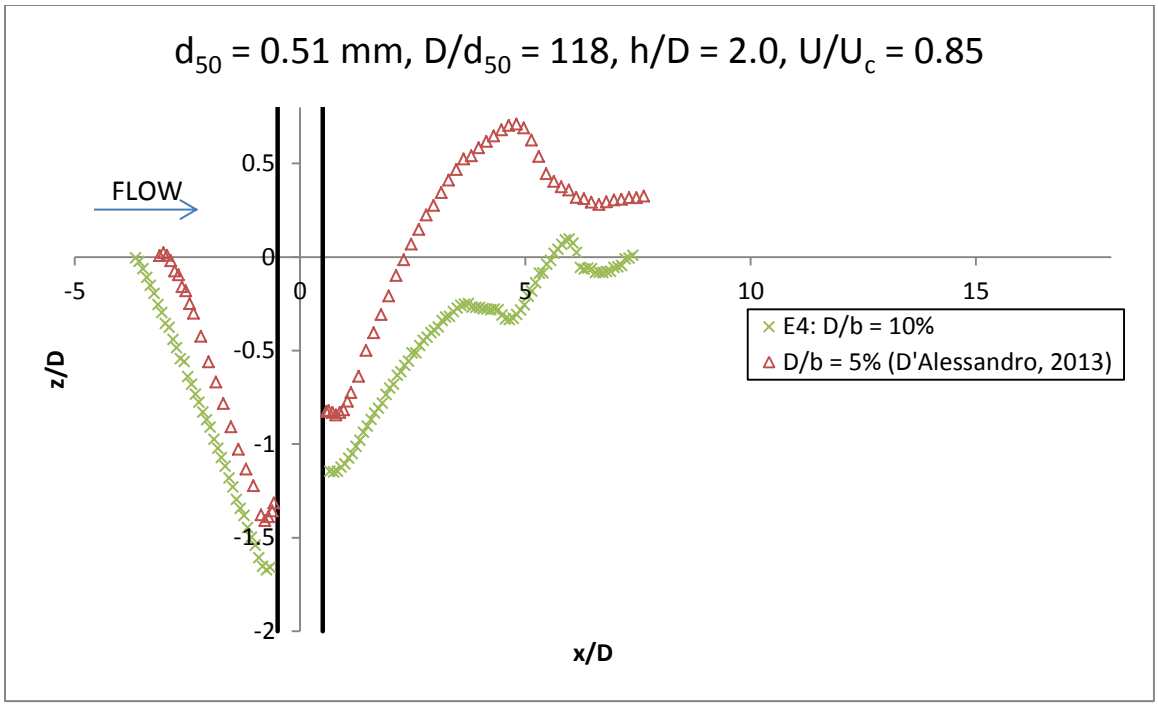

Figure 4.18. Comparison of centreline profiles for E4 with D'Alessandro's (2013) E16

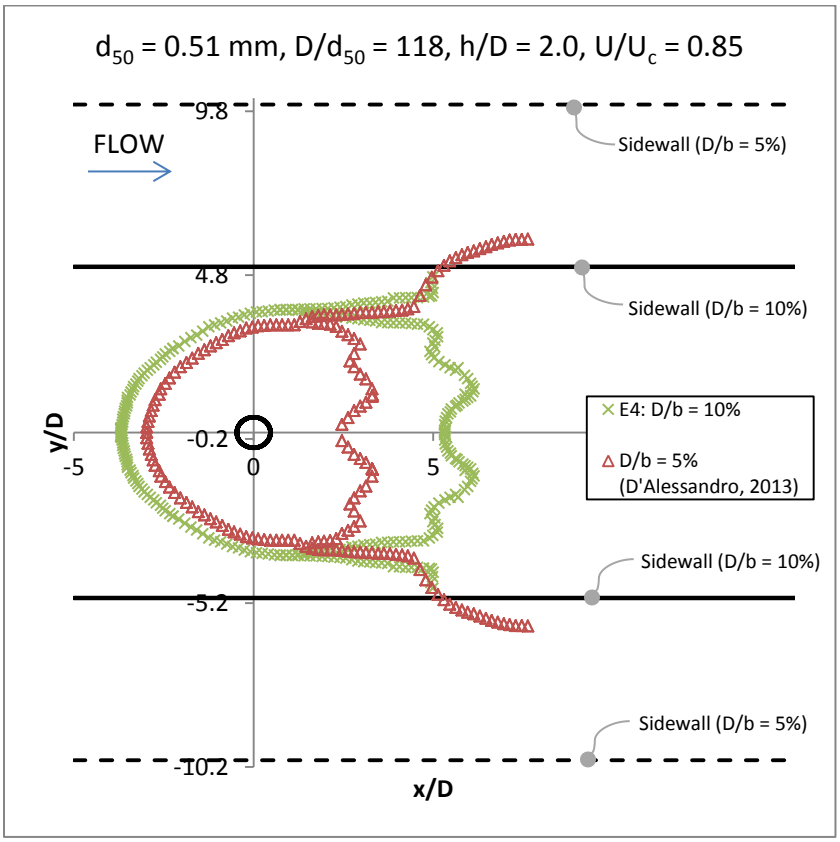

Figure 4.19. Comparison of contour profiles for E4 with D'Alessandro's (2013) E16

Figures 4.20 and **4.21** (below) compare scour profiles for test F4 and a test by Tejada (2014). All non-dimensional parameters for this pair of tests are constant, except for D/b, which is 15% in Tejada's test and 10% in E4. Densimetric Froude number is also identical between these two tests. These tests show that for d_{50} = 0.77 mm, there is a decrease in d_{se}/D with increasing blockage, as scour is lesser in Tejada's test with D/b = 15% than in E4 with D/b = 10%.

Scour also fails to reach the sidewalls despite a higher blockage ratio, extending downstream parallel to the walls. This contradicts the observations between test E4 and D'Alessandro's E16 (above), in which for tests with d_{50} = 0.51 mm, d_{se}/D increases with increasing D/b. These conflicting observations confirm the complexity of the scouring process, and highlight the difficulty which lies in isolating specific parameters for analytical purposes. However, F_d is lesser for the tests shown in **Figures 4.20** and **4.21** than for the tests shown in **Figures 4.17** through **4.19**, indicating that the effects of wall interference due to blockage may differ due to varying densimetric Froude number.

Figures 4.22 and **4.23** show a comparison of test F2 with two of Tejada's (2014) tests. For all three tests, D/d_{50}, h/D, and U/U_c are constant. Tejada's tests were performed in sediment with d_{50} = 0.51 mm, and F2 was performed in sediment with d_{50} = 0.77 mm. If Tejada's tests are viewed separately, then the observations from **Figures 4.17** through **4.19** (tests with varying blockage) are confirmed; in tests with higher blockage ratio, scour is deeper, wider, and longer, and reaches the sidewalls at a comparatively shorter length downstream. In fact, at a smaller blockage ratio (D/b = 5%), scour under these conditions failed to reach the sidewalls altogether.

Both profiles comparisons show that scour for test F2 (F_d = 2.30) is larger than for Tejada's tests (F_d = 2.40), despite one of Tejada's tests having higher blockage (15%) than F2 (10%). Therefore, the influences of densimetric Froude number on scour depth and geometry are greater than sidewall effects due blockage alone.

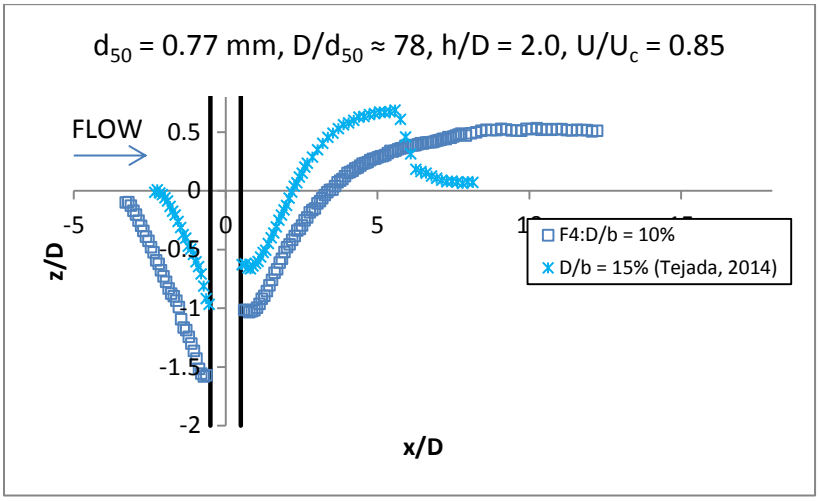

Figure 4.20. Comparison of centreline profiles for F4 and Tejada's (2014) Y4 test

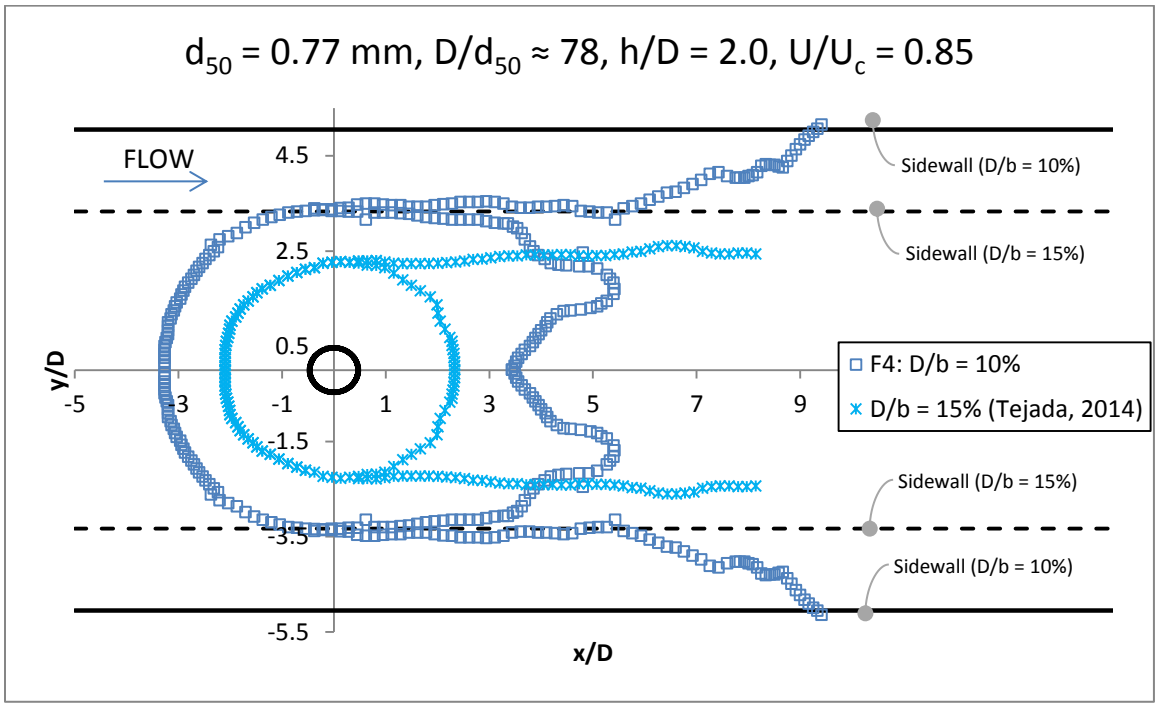

Figure 4.21. Comparison of contour profiles for F4 and Tejada's (2014) Y4 test

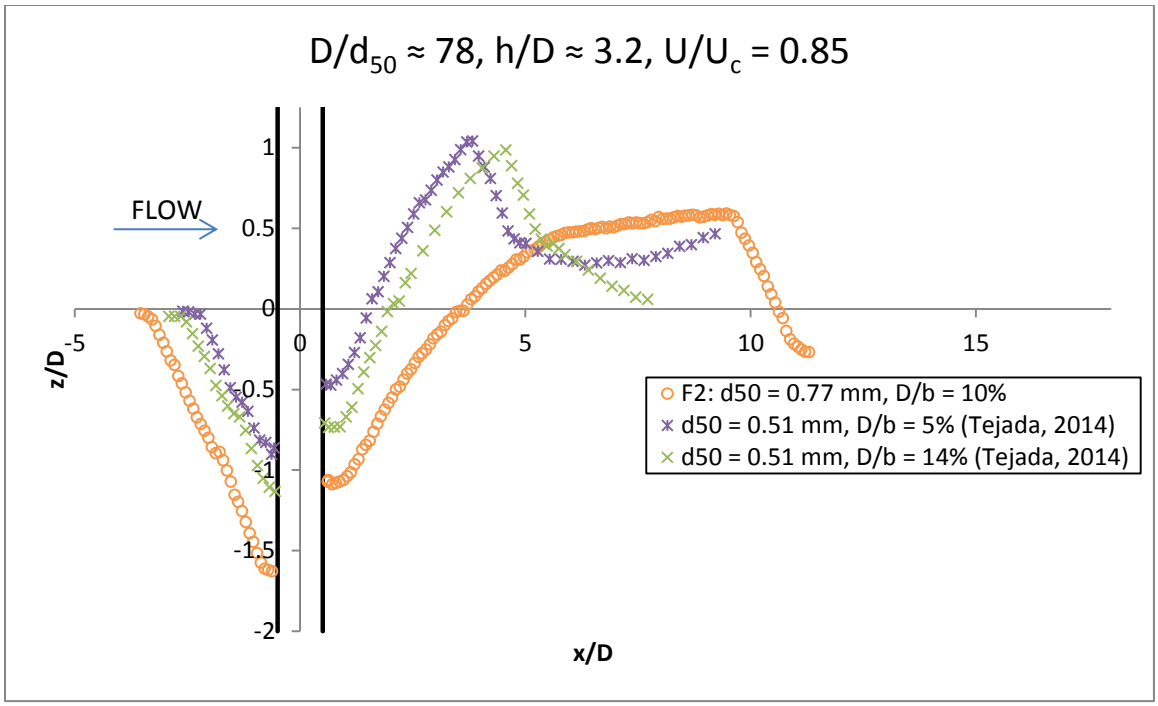

Figure 4.22. Comparison of centreline profiles for F2 and Tejada's (2014) C1 and W4

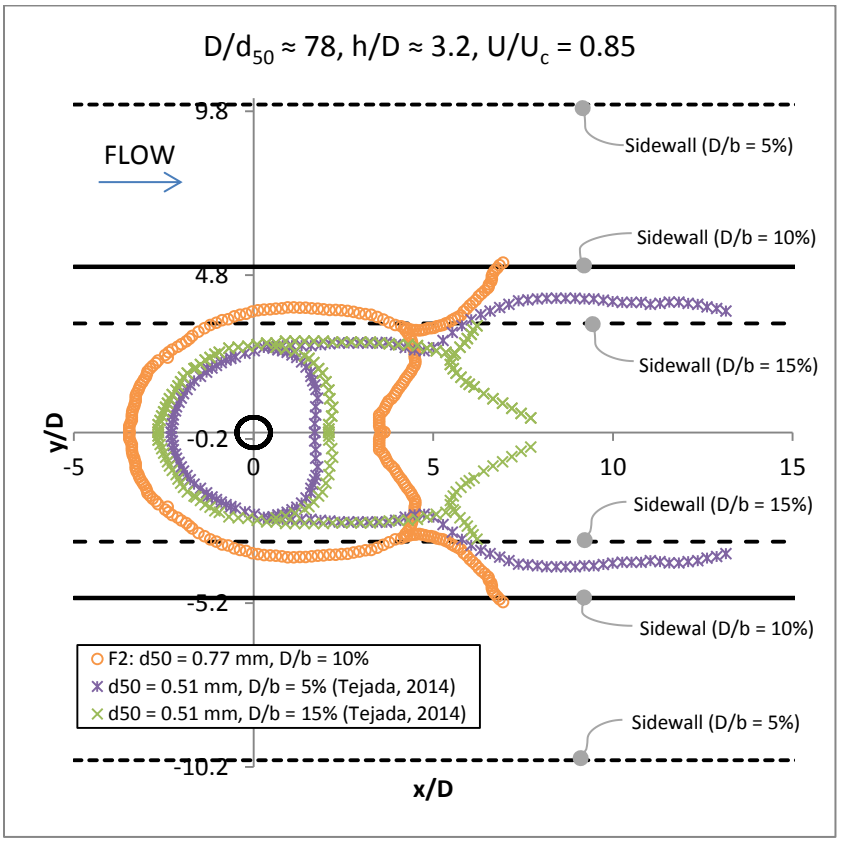

Figure 4.23. Comparison of contour profiles for F2 and Tejada's (2014) C1 and W4

4.5. Development of a New Scour Prediction Method

As previously discussed, the principal non-dimensional factors which are typically used in scour estimation methods are relative coarseness (D/d_{50}), flow shallowness (h/D), and flow intensity (U/U_c). However, the experimentation in this investigation has shown that even when all three quantities are held constant, there are two additional parameters which are shown to effect scouring action. The first of these is the densimetric Froude number, F_d, which is representative of flow-sediment interactions, and the second parameter is wall interference due to blockage, which can be important in laboratory-scale experiments.

Figure 4.24 shows the graphical relationship between d_{se}/D and D/d_{50} for several University of Windsor investigations (including series A and series B from the present study), as well as results from a study by Ettema et al. in 2006. The figure shows that while there is a decreasing trend between the two parameters, there is no distinct single curve upon which the data can be collapsed. There is a large amount of scatter in the relationship, which implies that there are other influencing parameters.

However, when grouped by values of densimetric Froude number, F_d (**Figure 4.25**), a trend tends to appear. At least part of the scatter in the data can be attributed to varying values of F_d, with d_{se}/D decreasing with even minimal changes in F_d. Since F_d is representative of flow-sediment interactions, it was chosen as a primary parameter for estimation of relative scour depth. Therefore, the relationship between d_{se}/D and F_d can be determined in terms of D/d_{50}, which indicates that while D/d_{50} may not be a governing parameter of the highest importance, it still has an influence on d_{se}/D, particularly when compared with other non-dimensional quantities.

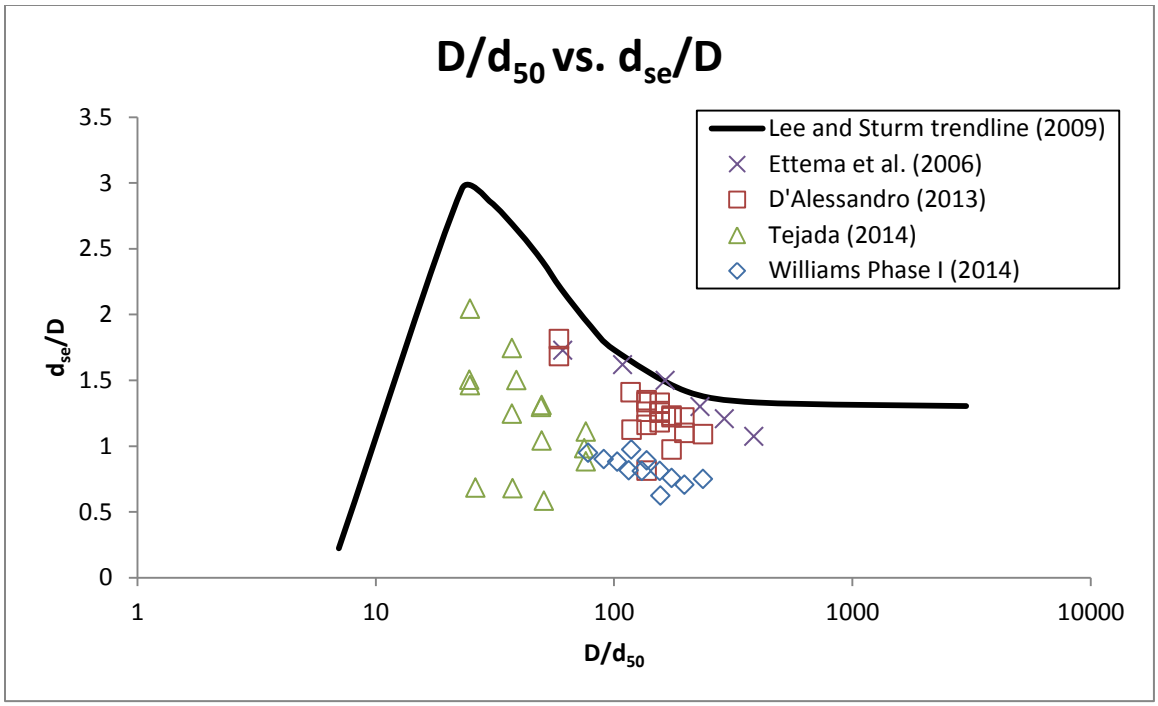

Figure 4.24. University of Windsor results with Ettema et al. (2006): D/d_{50} vs. d_{se}/D

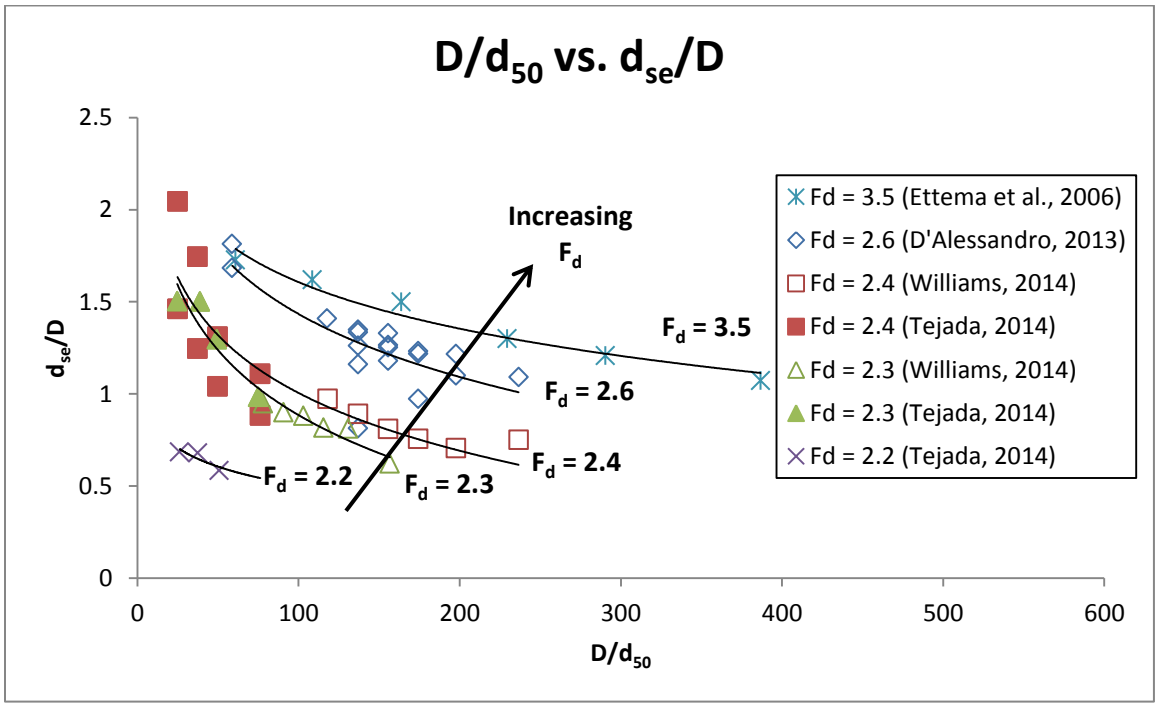

Figure 4.25. University of Windsor results with Ettema et al. (2006): D/d_{50} vs. d_{se}/D (by F_d)

Figure 4.26 shows the relationship between d_{se}/D and D/b, or blockage ratio, for the same University of Windsor investigations as **Figures 4.24** and **4.25**, in addition to

that of Ettema et al. (2006). As before, it is difficult to derive a meaningful relationship between d_{se}/D and wall interference by the use of D/b. Therefore, another parameter must exist which describes the propensity of increased blockage to increase wall interference in scouring action. This lies in the form of U_s, the separation velocity of flow (discussed above in **Section 4.1**). The influence of U_s is not only manifested in the form of increased flow velocity, but rather on the flow velocity near the pier itself. With increasing blockage, the pressure distribution around the pier is also increased or amplified (Ramamurthy, 1973), and U_s is a function of the base pressure coefficient at the downstream face of the pier.

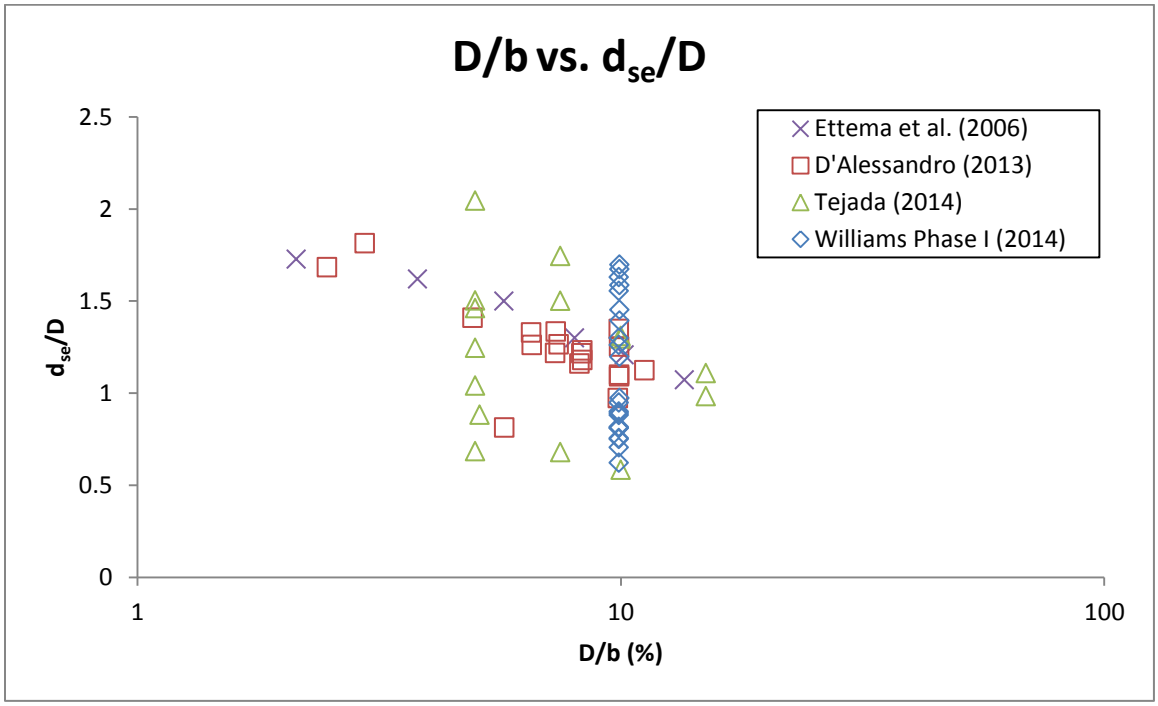

Figure 4.26. University of Windsor results with Ettema et al. (2006): D/b vs. d_{se}/D

Flow velocity in F_d was replaced with U_s, yielding the term F_{ds} (**Equation 4.2**), which was used for prediction of d_{se}/D; inclusion of this term would reduce scatter by accounting for a non-flow –intensity-related parameter representing flow-sediment

interactions, as well as incorporating a parameter which would account for the correction due to blockage.

$$F_{ds} = \frac{U_s}{\sqrt{g(SG-1)d_{50}}} \qquad \textbf{[4.2]}$$

As discussed in **Sections 4.2** and **4.3**, when isolated, relative coarseness and flow shallowness influences on relative scour depth are evident. Therefore, the three parameters used for estimation of d_{se} were chosen to be F_{ds}, h/D, and D/d_{50}. As the general trend of relationships between each parameter and d_{se}/D were exponential in nature, the form of the equation became

$$\frac{d_{se}}{D} = C(F_{ds})^{n_1}\left(\frac{h}{D}\right)^{n_2}\left(\frac{D}{d_{50}}\right)^{n_3} \qquad \textbf{[4.3]}$$

Here, C is a constant. The Solver tool in Microsoft Excel was used to determine the values of each exponent n and constant C of **Equation 4.3**, yielding **Equation 4.4**.

$$\frac{d_{se}}{D} = 1.010(F_{ds})^{-0.284}\left(\frac{h}{D}\right)^{0.325}\left(\frac{D}{d_{50}}\right)^{0.059} \qquad \textbf{[4.4]}$$

Figure 4.27 shows the graphical relationship between actual d_{se}/D and predicted d_{se}/D, (calculated using **Equation 4.4**), grouped by investigation. The equation does not tend towards over- or under-prediction of d_{se}/D, generating a reasonable trend along the line of perfect agreement (shown on the figure in black). **Figure 4.28** shows the relationship between actual and predicted d_{se}/D using (a) the S/M equation and (b) the HEC-18 equation. Both of these estimation methods significantly over-predict d_{se}/D, particularly when compared with **Equation 4.4**. In addition, **Figures 4.28[a]** and **4.28[b]** show more scatter than **Figure 4.27**.

In **Figures 4.27** and **4.28**, $(d_{se}/D)_m$ indicates the measured or actual value of scour, and $(d_{se}/D)_p$ denotes the predicted or calculated value of scour. Results from an investigation by Sheppard et al. (2004) on large-scale experimentation are included, as well as field measurements from various investigations, which were presented by Froehlich (1988).

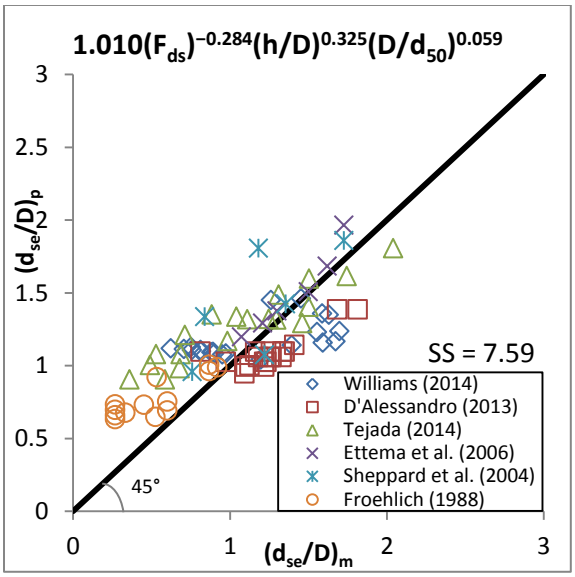

Figure 4.27. Actual vs. predicted d_{se}/D for all results grouped by investigation

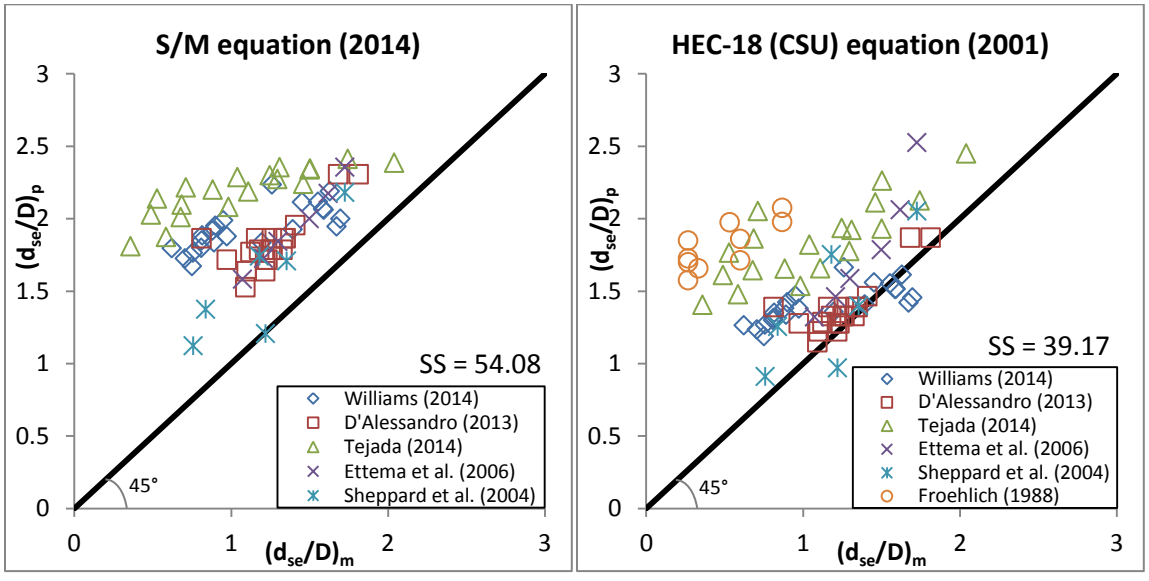

Figure 4.28. Measured vs. predicted d_{se}/D for the [a] S/M equation and [b] HEC-18 equation

In conclusion, **Equation 4.4** offers a reasonable estimate of d_{se}/D, particularly when compared with the Sheppard-Melville equation and the HEC-18 equation. While the HEC-18 equation had previously been determined to offer the most accurate prediction of d_{se}/D in large-scale tests (Williams et al., 2013), the correlation between $(d_{se}/D)_p$ calculated using **Equation 4.4** and $(d_{se}/D)_m$ (**Figure 4.27**) is stronger than the correlation between $(d_{se}/D)_p$ calculated using the HEC-18 equation and $(d_{se}/D)_m$ for Sheppard et al.'s (2004) large-scale tests and field measurements of scour presented by Froehlich (1988) (**Figure 4.28[a]**). The Sheppard-Melville equation was not used to predict d_{se}/D for field measurements, as it requires a value of U/U_c which was not available. It is important to note that **Equation 4.4** was derived mainly on the basis of University of Windsor results, for which U/U_c was maintained constant between 0.85 and 0.86, non-cohesive soils were used, and pier shape was circular.

CHAPTER 5

CONCLUSIONS AND RECOMMENDATIONS

5.1. Conclusions

In the past, many scour prediction methods have employed some combination of relative coarseness (D/d_{50}), flow shallowness (h/D), and flow intensity (U/U_c) to yield a design value of relative scour depth (d_{se}/D). These non-dimensional parameters are representative of interactions between the three main components of scour: flow, sediment, and structure. However, prior experimentation at the University of Windsor has shown that wall interference due to blockage ratio (D/b) also affects scour depth and geometry.

In this investigation, various parameter influences in scour experimentation were explored in order to develop a scour depth estimation method using results from the present investigation as well as results of two previous investigations on scour from the University of Windsor. Two phases of testing were carried out in order to investigate the effects of D/d_{50} and h/D on d_{se}/D. Experimental results were then compared with previously obtained results from other University of Windsor investigations in order to develop a new scour-predicting equation.

The following conclusions were drawn from this investigation:

- d_{se}/D decreases with increasing D/d_{50} until a limiting value of $D/d_{50} = 175$, after which d_{se}/D reaches a constant value of approximately 0.75, which is in agreement with Lee and Sturm's (2009) trendline
- d_{se}/D increases with increasing h/D for values above $h/D = 1.4$, until $h/D = 2.0$ to $h/D = 3.2$, over which range d_{se}/D is constant; however, d_{se}/D decreases again for

values of h/D > 3.2. Therefore, Melville and Coleman's (2000) trendline (for which d_{se}/D is constant for h/D > 1.4) is not valid when the influences of h/D are isolated

- In tests with similar values of D/d_{50} and constant h/D, D/b and U/U_c, densimetric Froude number (F_d) is shown to affect scour depth and geometry
- Similarly, variation in flow velocity at the point of separation around the pier (U_s) also affects scour, and is representative of wall interference from blockage effects
- A non-dimensional parameter (F_{ds}) was defined and incorporated into a new scour estimation method, representing flow-sediment interactions while also accounting for blockage effects

5.2. Recommendations

Recommendations for future investigations include expansion of testing on flow shallowness; phase II testing from the present investigation should be replicated in beds of various sediment size. More importantly, testing should be completed for a large range of h/D values, particularly those greater than 4 (which was the maximum value of h/D that the present investigation was able to achieve), with all other non-dimensional quantities of importance (D/d_{50}, D/b, U/U_c, F_d, etc.) held constant in order to isolate for its effects. These two recommended phases of testing could then be used to further investigate the influence of the densimetric Froude number on scour. The newly proposed equation may also undergo expanded analysis; for example, its applicability to field results should be further explored. Finally, scour modelling using computational fluid dynamics (CFD) should also be explored in order to refine the proposed equation for design purposes.

REFERENCES

1. American Association of State Highway and Transportation Officials (2012). "AASHTO LRFD Bridge Design Specifications." American Association of State and Highway Transportation Officials, Washington, D.C.

2. Beg, M. (2010). "Characteristics of Developing Scour Holes around Two Piers Placed in Transverse Arrangement." Scour and Erosion: 76-85.

3. Breusers, H.N.C., Nicollet, G., and Shen, H.W. (1977). "Local Scour Around Cylindrical Piers." Journal of Hydraulic Research, 15(3), 211-252.

4. Chiew, Y. (1984). "Local Scour at Bridge Piers." Ph.D Thesis, Auckland: School of Engineering, University of Auckland, New Zealand.

5. CSA International, Standards Council of Canada (2006). "Canadian Highway Bridge Design Code, CAN/CSA-26-06." Canadian Standards Association, Toronto, ON.

6. CTV News. (2013, June 27). "Calgary bridge failure caused by flooding." CTV News. Retrieved February 28, 2014, from www.ctvnews.ca.

7. D'Alessandro, C. (2013). "Effect of Blockage on Circular Bridge Pier Local Scour." M.A.Sc. Thesis, Faculty of Engineering, University of Windsor, Canada.

8. Debnath, K. and Chaudhuri, S. (2010). "Bridge Pier Scour in Clay-Sand Mixed Sediments at Near-Threshold Velocity for Sand." Journal of Hydraulic Engineering, 136(9), 597-609.

9. Deng, L. and Cai, C. (2010). "Bridge Scour: Prediction, Modeling, Monitoring, and Countermeasures—Review." Practice Periodical on Structural Design and Construction, 15(2), 125–134.

10. Dey, S., Bose, S., and Sastry, G. (1995). "Clear Water Scour at Circular Piers: a Model." Journal of Hydraulic Engineering, 121(12), 869–876.

11. Diab, R., Link, O., and Zanke, U. (2010). "Geometry of Developing and Equilibrium Scour Holes at Bridge Piers in Gravel." Canadian Journal of Civil Engineering, 37(4), 544-552.

12. Ettema, R., Melville, B., and Barkdoll, B. (1998). "Scale Effects in Pier-Scour Experiments." Journal of Hydraulic Engineering, 124(6), 639–642.

13. Ettema, R., Kirkil, G., and Muste, M. (2006). "Similitude of Large-Scale Turbulence in Experiments on Local Scour at Cylinders." Journal of Hydraulic Engineering, 132(1), 33–40.

14. Ettema, R., Constantinescu, G., and Melville, B. (2011). "NCHRP Web-Only Document 175: Evaluation of Bridge Scour Research: Pier Scour Processes and Predictions." From [http://onlinepubs.trb.org/onlinepubs/nchrp/nchrp_w175.pdf]

15. Figliola, R.S. and Beasley, D.E. (2011). Theory and Design for Mechanical Measurements: Fifth Edition. USA: John Wiley & Sons, Inc.

16. Foti, S. and Sabia, D. (2011). "Influence of Foundation Scour on the Dynamic Response of an Existing Bridge." Journal of Bridge Engineering, 16(2), 295–304.

17. Froehlich, D. (1988). "Analysis of On-site Measurements of Scour at Piers." Proceedings of the 1988 ASCE National Hydraulic Engineering Conference, Colorado Springs, CO: ASCE.

18. Guo, J. (2012). "Pier Scour in Clear Water for Sediment Mixtures." Journal of Hydraulic Research, 50(1), 18-27.

19. Heller, V. (2011). "Scale Effects in Physical Hydraulic Engineering Models." Journal of Hydraulic Research, 49(3), 293-306.

20. Hodi, B. (2009). "Effect of Blockage and Densimetric Froude Number on Circular Bridge Pier Scour." M.A.Sc. Thesis, Faculty of Engineering, University of Windsor, Canada.

21. Jain, S C. (1981). "Maximum Clear-Water Scour around Circular Piers." Journal of the Hydraulics Division, 107(5), 611-626.

22. Johnson, P. and Torrico, E. (1994). "Scour around wide piers in shallow water." Transportation Research Record, (1471), 66-70.

23. Khwairakpam, P. and Mazumdar, A. (2009). "Local Scour Around Hydraulic Structures." International Journal of Recent Trends in Engineering, 1(6), 59-61.

24. Lai, J., Chang, W., and Yen, C. (2009). "Maximum Local Scour Depth at Bridge Piers under Unsteady Flow." Journal of Hydraulic Engineering,135(7), 609–614.

25. Laursen M.E., and Toch, A. (1956). "Scour Around Bridge Piers and Abutments." Bulletin No. 4, Iowa Institute of Hydraulic Research.

26. LeBeau, K. and Wadia-Fascetti, S. (2007). "Fault Tree Analysis of Schoharie Creek Bridge Collapse." Journal of Performance of Constructed Facilities., 21(4), 320–326.

27. Lee, S. and Sturm, T. (2009). "Effect of Sediment Size Scaling on Physical Modeling of Bridge Pier Scour." Journal of Hydraulic Engineering, 135(10), 793–802.

28. Melville, B., and Coleman, S. (2000). Bridge Scour. Colorado: Water Resources Publications.

29. Melville, B., and Sutherland, A. (1988). "Design Method for Local Scour at Bridge Piers." Journal of Hydraulic Engineering, 114(10), 1210–1226.

30. Melville, B., and Chiew, Y. (1999). "Time Scale for Local Scour at Bridge Piers." Journal of Hydraulic Engineering, 125(1), 59–65.

31. Miroff, N. (2007, August 3). "Collapse Spotlights Weaknesses in U.S. Infrastructure." *Washington Post*, Nation, www.washingtonpost.com [accessed November 2012]

32. National Cooperative Highway Research Program (2011). "NCHRP No. 682: Scour at Wide Piers and Long Skewed Piers." Sheppard, D., Demir, H., Melville, B. From [http://onlinepubs.trb.org/onlinepubs/nchrp/nchrp_rpt_682.pdf]

33. Norberg, C. (1987). "Effects of Reynolds Number and a Low-Intensity Freestream Turbulence on the Flow around a Circular Cylinder." Dept. of Appl. Thermodynamics and Fluid Mech., Chalmers Univ. of Tech., Gothenburg, Sweden, Publ, (87/2).

34. Ontario Ministry of Transportation, Quality and Standards Division (1991). Ontario Highway Bridge Design Code, 3rd edition.

35. Raikar, R V. and Dey, S.(2009). "Maximum Scour Depth at Piers in Armor-beds." KSCE Journal of Civil Engineering, 13(2), 137-142.

36. Ramamurthy, A S. (1973). "Wall Effects on Flow Past Bluff Bodies." Journal of Sound and Vibration, 31(4), 443-51.

37. Richardson, E., Simons, Julien, P. (1990). "Highways in the River Environment, FHWA-HI-90-016." Federal Highway Administration, U.S. Department of Transportation, Washington, D.C.

38. Richardson, E., and Davis, S. (2001). "Evaluating Scour at Bridges," Fourth Edition. Federal Highway Administration, Washington, D.C.

39. Roshko, A. (1961). "Experiments on the Flow past a Circular Cylinder at Very High Reynolds Number." Journal of Fluid Mechanics, 10(03), 345-356.

40. Sheppard, D., Odeh, M., and Glasser, T. (2004). "Large Scale Clear-Water Local Pier Scour Experiments." Journal of Hydraulic Engineering, 130(10), 957–963.

41. Sheppard, D. and Miller, W. (2006). "Live-Bed Local Pier Scour Experiments." Journal of Hydraulic Engineering, 132(7), 635–642.

42. Sheppard, D., Melville, B., and Demir, H. (2014). “Evaluation of Existing Equations for Local Scour at Bridge Piers.” Journal of Hydraulic Engineering, 140(1), 14–23.

43. Shirhole, A.M. and Holt, R.C. (1991). “Planning for a Comprehensive Bridge Safety Program.” Transportation Research Record 1290, Transportation Research Board, National Research Council, Washington, D.C., 1, 39-50.

44. Sumer, B.M., and Fredsoe, J. (2002). Advanced Series on Ocean Engineering, Volume 17: The Mechanics of Scour in the Marine Environment. Singapore: World Scientific Publishing.

45. Tejada, S. (2013). “Effects of Blockage and Relative Coarseness on Clear Water Bridge Scour.” M.A.Sc. Thesis, Faculty of Engineering, University of Windsor, Canada

46. Wardhana, K. and Hadipriono, F. (2003). “Analysis of Recent Bridge Failures in the United States.” Journal of Performance of Constructed Facilities, 17(3), 144–150. Edition. Ontario Ministry of Transportation, Quality and Standards Division, Toronto, ON.

47. Williams, P., Balachandar, R., and Bolisetti, T. (2013). “Evaluation of Local Bridge Pier Scour Depth Estimation Methods.” Proceedings of the 24th Canadian Congress of Applied Mechanics held in Saskatoon, SK, Canada, 2-6 June 2013

APPENDICES

Appendix A: Summary of Experimental Results

Test ID	D (m)	d_{50} (mm)	h (m)	b (m)	U (m/s)	d_s (cm)	d_s/D	w_s (cm)	w_s/D	Fr	U/U_c (m/s)	D/b	h/D	D/d_{50}	Re
A1	0.121	0.51	0.193	1.22	0.224	7.62	0.632	49.4	4.09	0.162	0.85	0.1	1.6	237	2.7E+04
A2	0.101	0.51	0.161	1.02	0.224	7.12	0.706	41.4	4.11	0.178	0.85	0.1	1.6	198	2.3E+04
A3	0.089	0.51	0.142	0.90	0.224	6.73	0.757	36.7	4.13	0.189	0.85	0.1	1.6	174	2.0E+04
A4	0.079	0.51	0.127	0.80	0.224	6.43	0.810	32.7	4.12	0.200	0.85	0.1	1.6	156	1.8E+04
A5	0.070	0.51	0.112	0.71	0.224	6.23	0.892	32.2	4.61	0.213	0.85	0.1	1.6	137	1.6E+04
A6	0.060	0.51	0.096	0.61	0.224	5.87	0.974	29.4	4.88	0.230	0.85	0.1	1.6	118	1.3E+04
B1	0.121	0.77	0.193	1.22	0.259	7.51	0.622	43.4	3.60	0.188	0.85	0.1	1.6	157	3.1E+04
B2	0.101	0.77	0.161	1.02	0.259	8.18	0.812	43.5	4.32	0.206	0.85	0.1	1.6	131	2.6E+04
B3	0.089	0.77	0.142	0.90	0.259	7.26	0.817	37.9	4.26	0.219	0.85	0.1	1.6	115	2.3E+04
B4	0.079	0.77	0.127	0.80	0.259	7.00	0.882	35.4	4.46	0.232	0.85	0.1	1.6	103	2.1E+04
B5	0.070	0.77	0.112	0.71	0.259	6.29	0.901	32.9	4.71	0.247	0.85	0.1	1.6	91	1.8E+04
B6	0.060	0.77	0.096	0.61	0.259	5.70	0.946	26.6	4.41	0.266	0.85	0.1	1.6	78	1.6E+04
E1	0.060	0.51	0.240	0.61	0.224	8.75	1.452	42.3	7.02	0.146	0.85	0.1	4.0	118	1.3E+04
E2	0.060	0.51	0.192	0.61	0.224	9.56	1.587	48.0	7.97	0.163	0.85	0.1	3.2	118	1.3E+04
E3	0.060	0.51	0.144	0.61	0.224	10.23	1.698	48.4	8.03	0.188	0.85	0.1	2.4	118	1.3E+04
E4	0.060	0.51	0.120	0.61	0.224	10.08	1.673	44.0	7.30	0.206	0.85	0.1	2.0	118	1.3E+04
E5	0.060	0.51	0.112	0.61	0.224	8.40	1.394	39.0	6.47	0.213	0.85	0.1	1.9	118	1.3E+04
E6	0.060	0.51	0.085	0.61	0.224	7.21	1.197	34.2	5.68	0.245	0.85	0.1	1.4	118	1.3E+04
F1	0.060	0.77	0.241	0.61	0.259	7.57	1.260	32.4	5.38	0.168	0.85	0.1	4.0	78	1.6E+04
F2	0.060	0.77	0.193	0.61	0.259	9.78	1.623	44.6	7.40	0.188	0.85	0.1	3.2	78	1.6E+04
F3	0.060	0.77	0.145	0.61	0.259	9.33	1.549	43.0	7.14	0.217	0.85	0.1	2.4	78	1.6E+04
F4	0.060	0.77	0.120	0.61	0.259	9.55	1.585	40.8	6.77	0.239	0.85	0.1	2.0	78	1.6E+04
F5	0.060	0.77	0.096	0.61	0.259	5.70	0.946	26.6	4.41	0.266	0.85	0.1	1.6	78	1.6E+04

VITA AUCTORIS

NAME:	Priscilla Williams
PLACE OF BIRTH:	Kingston, ON
YEAR OF BIRTH:	1989
EDUCATION:	Vincent Massey Secondary School, Windsor, ON, 2007
	University of Windsor, B.A.Sc., Windsor, ON, 2011
	University of Windsor, M.A.Sc., Windsor, ON, 2014
MEMBERSHIP:	Professional Engineers Ontario (E.I.T), ON, 2012